Lumped fiber Raman amplifiers with highly nonlinear fiber

Hui Zhang

A Thesis

In

The Department of Electrical and Computer Engineering

Presented in Partial Fulfillment of the Requirements

for the Degree of Master of Applied Science at

Concordia University

Montreal, Quebec, Canada

Your file Votre référence
ISBN: 0-494-14289-8
Our file Notre référence
ISBN: 0-494-14289-8

ABSTRACT

Lumped fiber Raman amplifiers with highly nonlinear fiber

Hui Zhang

Fiber Raman amplifiers (FRAs) can provide broadband and low-noise-figure amplification, and the gain can be achieved at any wavelength. It has been proved that FRA is a useful technique to extend the span lengths and capacity of fiber-optic transmission systems.

In particular, lumped fiber Raman amplifiers (LRAs), based on dispersion compensating fibers, have been considered in long-haul WDM transmission systems. However, noise can limit the performance of LRAs having a gain of more than 15 dB. Noise degrades the optical signal-to-noise ratio (OSNR) resulting in receiver sensitivity penalty and thus the amplifier gain is limited to some extent for a single LRA.

Highly nonlinear fiber (HNLF) is a fiber with high nonlinearity to generate Raman gain efficiently and can be used as a gain medium for lumped Raman amplifiers. In this thesis, we will investigate Raman gain and noise characteristics of LRAs using HNLFs as a gain medium. It is shown that both the signal and the amplified spontaneous emission induced multiple-path interferences are suppressed in LRAs with HNLF, thus for the same Raman gain a better noise performance can be achieved independently of co-, counter- and bi- directional pumping methods, compared to LRAs with DCF gain medium. Moreover, the effect of Rayleigh scattering coefficient on LRA's noise performance improvement is also investigated.

To achieve an accurate modeling, a theoretical model, which includes effects of multiple-path interference (MPI), anti-Stokes, and Rayleigh scattering, is used, and a new Raman gain coefficient scaling method is also employed in this modeling.

ACKNOWLEDGMENTS

I would like to express my great thanks to my research advisor Professor John X. Zhang for his support and guidance over the past two years. His high expectations and enlightening advices have helped me improve, and made this thesis possible. I am also grateful to Guodong Zhang, AT&T USA, for his time and help.

PUBLICATION RELATED TO THIS WORK

1. Hui Zhang, Xiupu Zhang, Guodong Zhang, "Noise performance improvement of lumped fiber Raman amplifiers using highly nonlinear fiber," submitted to Optics Express, Oct. 2005.

TABLE OF CONTENTS

LIST OF FIGURES

LIST OF TABLES

ACRONYMS

ASE	Amplified Spontaneous Emission
CWDM	Coarse WDM
DCF	Dispersion Compensating Fiber
DWDM	Dense WDM
EDFA	Erbium-doped Fiber Amplifier
FRA	Fiber Raman Amplifier
FWM	Four Wave Mixing
HNLF	Highly Nonlinear Fiber
LEAF	Large Effective Area Fiber
LRA	Lumped Fiber Raman Amplifier
MPI	Multiple-path Interference
PCF	Photonic Crystal Fiber
PMD	Polarization-mode Dispersion
SBS	Stimulated Brillion Scattering
SMF	Standard Single Mode Fiber
SOA	Semiconductor Optical Amplifier
SRS	Stimulated Raman Scattering
SPM	Self-phase Modulation
WDM	Wavelength-division Multiplexed
XPM	Cross-phase Modulation

CHAPTER 1 Introduction

This chapter will explain the background, origin, and targets of this thesis. The optical fiber Raman amplifier is introduced in Section 1.1, including its brief history, functions, and developments. The project is explained in Section 1.2, including the basic idea of this project and a list of works to be done. The thesis structure and contents are given in Section 1.3.

1.1 Fiber Raman Amplifier (FRA) review

Fiber-optic communication systems are also called light-wave systems because they employ optical fibers to transmit information. The first generation of light-wave systems became commercially available in 1980. Since then, fiber-optic communication systems have been deployed worldwide.

The role of a communication channel is to transport the optical signal from the transmitter to the receiver without distorting it. Most light-wave systems use optical fibers as the communication channel because silica fibers can transmit light with losses as small as 0.2dB/km. The transmission distance of any optical transmission system is eventually limited by fiber losses that are caused by material absorption, Rayleigh scattering, and wave-guide imperfections.

For long-haul systems, optoelectronic repeaters were used to solve the problem originated from the fiber loss. Since optoelectronic repeaters need to convert the optical signal into electric signal at first, and then the optical signal is regenerated before re-transmitting, they become inevitably complex and expensive for wavelength-division multiplexed (WDM) light-wave systems [1].

An alternative approach to loss management makes use of optical amplifiers, which amplify the optical signal directly without requiring its conversion to the electric domain. Several kinds of optical amplifiers were developed during the 1980s including the

semiconductor optical amplifiers (SOAs), the erbium-doped fiber amplifiers (EDFAs), and the fiber Raman amplifiers (FRAs). The use of optical amplifiers became widespread during the 1990s [2].

SOA has a small form factor and can be integrated with other functions on an InP substrate. However, SOA is inherently non-linear. SOA's non-linearities cause crosstalk between channels, and crosstalk between bits (TDM crosstalk). Furthermore, because SOAs have a relatively low saturated output power, they have problems of high noise figure and polarization sensitivity. EDFA is the commonly used optical amplifier in recent optical communication systems. But EDFAs have narrow gain bandwidth due to their fluorescence spectra.

There has been an increasing interest in FRAs, which extends the usable optical bandwidths by optimizing the pumping lightwave spectrum. By using FRAs, loss-free transmission can be achieved over a seamless bandwidth higher than 100 nm without rare-earth-doped fiber amplifiers and MUX/DEMUX devices, resulting into realization of low cost systems [3].

Research on Raman amplification in optical fibers started early in the 1970s [4]. The benefits from Raman amplification in the transmission fiber have already been investigated in the mid-1980s [5]. However, since FRAs need high pump power, it was only until the mid-1990s, with the development of suitable high-power pumps, that the FRAs regained interest. Figure 1.1 shows the number of published papers and submitted US patents in EDFAs and FRAs every year since 1980 [6].

Compared to SOAs and EDFAs, FRAs can work in any wavelength region. That is because the amplification factor is decided by the frequency difference between the pump and the signal only, not by the energy level difference of a rare earth ion, which is the case for EDFAs. FRAs also have good noise performance and can be used as distributed amplifiers.

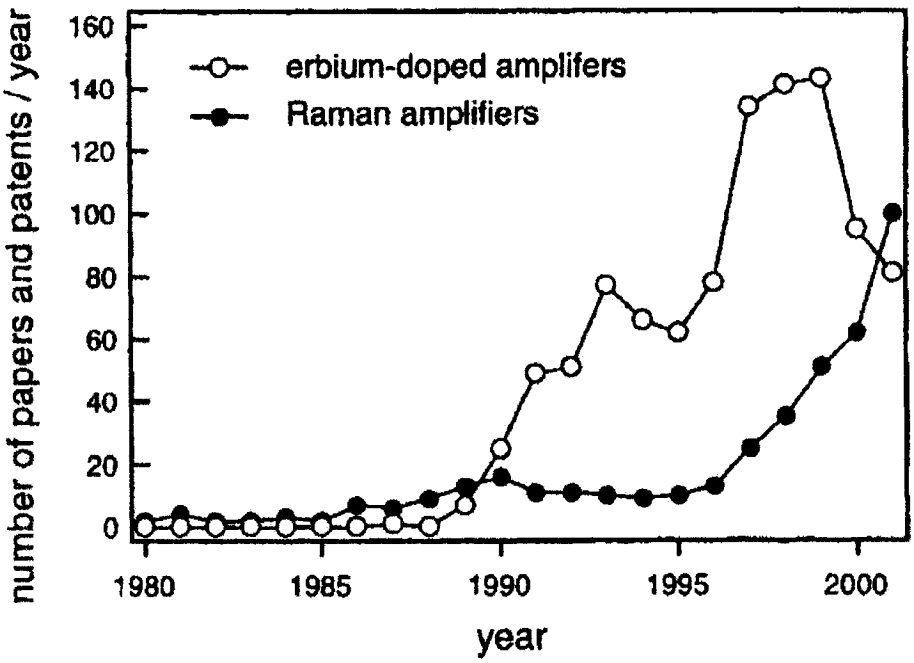

Figure 1.1 Number of published papers (conferences and journals of the OSA and IEEE) and submitted U.S. patents each year since 1980 in the fields of EDFAs and FRAs.

FRAs are attractive for DWDM transmission systems due to their advantages of broad amplification bandwidth and flexible central wavelength. With recent developments of optical pump sources with high power near 1400 nm wavelength and highly nonlinear fiber (HNLF) having a peak effective Raman gain coefficient more than ten times that of conventional single-mode fiber, FRAs are emerging as a practical optical amplifier technology, especially for opening new wavelength windows such as the short and ultra-long wavelength bands [7].

1.2 Aim of this thesis

This thesis is aimed at studying the gain and noise performance of lumped fiber Raman amplifiers (LRAs) with highly nonlinear fiber as a Raman gain medium.

FRAs have attracted great attention for their application in high-capacity long-haul dense wavelength division multiplexing transmission systems (DWDM) due to the improved optical signal to noise ratio (OSNR) and reduced fiber nonlinear impairments

[2, 6-10]. In particular, LRAs based on dispersion compensating fibers (DCFs), have been investigated for potential applications in broad-band WDM transmission systems. However, it was found that multiple path interference (MPI), mainly consisting of double Rayleigh scattering (DRS), induced by Rayleigh backscattering, can limit the performance of LRAs with DCF having a gain of ~15 dB and beyond [10]. For a Raman gain of beyond 15 dB, MPI or DRS will considerably degrade noise performance of LRAs, resulting in increased noise figure and worse optical signal-to-noise ratio (OSNR). Or rather, OSNR decreases rapidly with gain increase and thus the amplifier gain is limited to some extent for a single LRA.

Highly nonlinear fiber (HNLF) is a fiber specially designed for high nonlinearity, which can generate Raman gain efficiently and can be used as a Raman gain medium for LRAs [3, 7, and 8]. This kind of HNLF can have a normalized Raman gain efficiency g_R/A_{eff} of up to $7.2(W \cdot km)^{-1}$, and a twice larger ratio of g_R/A_{eff} to loss at the pump wavelength compared to DCFs [3, 8]. Therefore, it is expected that for the same Raman gain, LRAs can be implemented with a much shorter length of HNLFs compared to DCFs. Hence, for LRAs with HNLF or DCF having the same gain, MPI may be reduced when HNLFs are used because the HNLF length is much shorter than DCFs. Particularly, for a high Raman gain LRAs with HNLFs will have a better noise performance because that MPI, which is a dominant factor in noise performance, is expected to be reduced. Moreover, experimental measurements showed that noise performance is improved in fiber Raman amplifiers with standard single-mode fiber connected to a short length of highly nonlinear photonic crystal fiber (PCF) [12]. This suggests that noise suppression in Raman amplification is induced in HNLFs. However, Raman amplification with noise performance in HNLFs has not been investigated in detail, particularly compared to the conventional gain mediums of DCFs.

In this report, we study Raman gain and noise characteristics of LRAs using HNLF as a Raman gain medium. We will show that, in LRAs with HNLF, Raman gain can be

generated with a short length of fiber and MPI or DRS induced noise is significantly suppressed, resulting in a better noise performance compared to DCFs.

1.3 Thesis structure

Chapter 2 is to introduce the principle of FRAs. In the first part, stimulated Raman scattering is explained. An example illustrates how a fiber is used as a LRA, and properties to be noticed in Raman amplifier design are given. The second part describes the scaling of Raman gain coefficients. The relationship between Raman gain coefficients, pump wavelength, and effective area is given followed by an example.

Chapter 3 is to introduce the fiber Raman amplifier model we used in this thesis. Basic definitions are given to describe a FRA model. A theoretical model is constructed by the basic equation that is used to calculate the power of each channel. Calculations of ASE and MPI noise are also explained in this chapter. The model's accuracy is verified by comparing it to published experimental results.

In Chapter 4, we will show the fiber parameters used in our simulations, followed by an introduction to Rayleigh scattering coefficient. The Rayleigh scattering coefficient value used in this thesis was determined by repeating published experiments.

Chapter 5 is the main body of this thesis. Performance of LRAs with one pump is studied in this chapter. Eight investigations cases from different points of view are conducted. Conclusions are drawn from the comparison results between LRAs with HNLF and LRAs with conventional DCF.

In Chapter 6, performance comparisons are given between LRAs with multiple wavelength pumps and signal spectrum over C+L band. This is a spread of Chapter 5 and more close to real cases. We study LRAs with 2 or 4 wavelengths counter pumps and three cases are investigated in this chapter.

We investigate the impact of Rayleigh scattering coefficient on LRA's noise performance in Chapter 7. HNLF's Rayleigh scattering value is increased step by step to

study its effect on the amplifier's noise performance.

Chapter 8 concludes this thesis and sums up all the results shown in previous chapters. More discussions and possible future developments are also given in this chapter.

CHAPTER 2 Fiber Raman Amplifier Principle

A fiber-based raman amplifier uses stimulated raman scattering (SRS) occurring in silica fibers when an intense pump beam propagates throuth it. SRS, which is changed from spontaneous Raman scattering when the injected power exceeds a threshold value, is described in Section 2.1. Section 2.2 gives an example of how a fiber can be used as a FRA, and properties to be understood in FRA design. Raman gain coefficient scaling is the topic of Section 2.3, including explanation of Raman gain coefficients, relationship among these coefficients, pump wavelength, and effective area, and how to use this relation equation.

2.1 Raman amplification

A fiber-based Raman amplifier uses SRS occurring in silica fibers when an intense pump beam propagates through it. [1]

SRS was first discovered by Raman, for which he received the Nobel Prize in physics in 1930 [12]. Spontaneous Raman scattering occurs in optical fibers when a pump wave is scattered by the silica molecules. Some pump photons give up their energy to create other photons of reduced energy at a lower frequency; the remaining energy is absorbed by silica molecules, which end up in an excited vibrational state. The vibrational energy levels of silica dictate the value of the Raman shift $\Omega_R = \omega_p - \omega_s$. As an acoustic wave is not involved, spontaneous Raman scattering is an isotropic process and occurs in all directions.

In a solid-state quantum mechanical description, optical photons are inelastically scattered by quantized molecular vibrations called optical *phonons*. Photon energy is lost (the molecular lattice is heated) or gained (the lattice is cooled), shifting the frequency of the light. The components of scattered light that are shifted to lower frequencies are called Stokes lines; those shifted to higher frequencies, called anti-Stokes lines. The

frequency shift is equal to the oscillation frequency of the lattice phonon that is created or annihilated. (The anti-Stokes process is not mentioned further here as it is typically orders of magnitude weaker than the Stokes process in the context of optical communications, making it irrelevant.) Raman scattering can occur in all materials, but in silica glass the dominant Raman lines are due to the bending motion of the Si-O-Si bond [12].

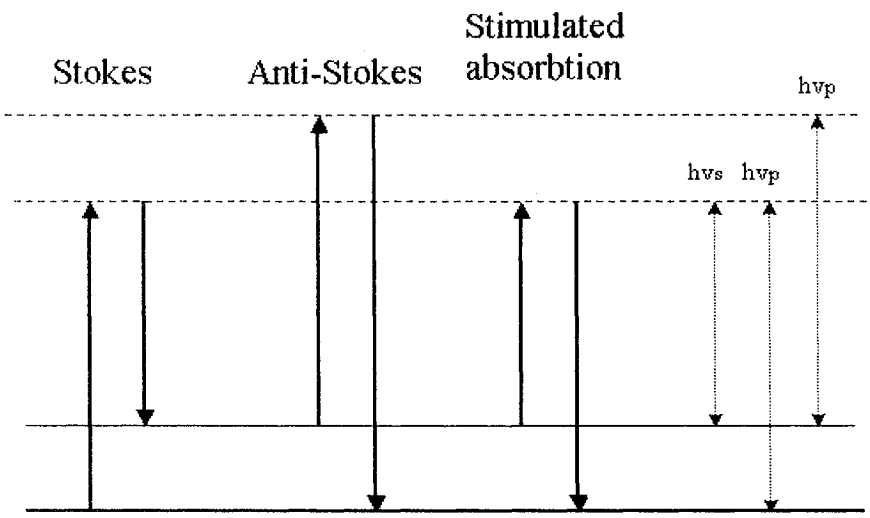

Figure 2.1 Energy diagram for the Raman scattering processes: Stokes scattering, anti-Stokes scattering and stimulated absorption. The energy differences between the levels are shown with dashed vertical lines on the right of the figure. The dashed horizontal lines show virtual levels.

Raman scattering can also be stimulated by signal light at an appropriate frequency shift from a pump, leading to stimulated Raman scattering. In this process, pump and signal light are coherently coupled by the Raman process. In a quantummechanical description, a pump photon is converted into a second signal photon that is an exact replica of the first, and the remaining energy produces an optical phonon. The initial signal photon, therefore, has been amplified. This process is considered nonresonant because the upper state is a short-lived virtual state [12].

2.2 Fiber Raman amplifiers

Figure 2.2 illustrates how a fiber works as a Raman amplifier [1]. The pump and signal beams at frequencies ω_p and ω_s are injected into the fiber through a fiber coupler. The energy is transferred from the pump beam to the signal beam through SRS as the two beams copropagate inside the fiber [1]. Therefore, the signals are amplified. At the output end, a filter is used to filter out the desired signal.

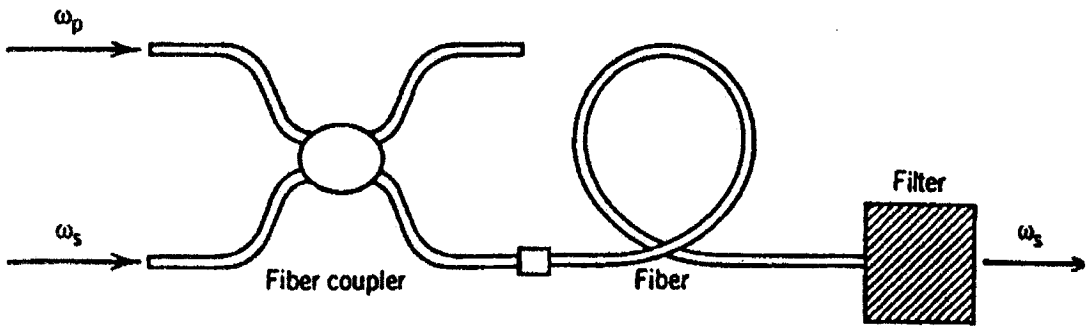

Figure 2.2 Schematic of a fiber-based Raman amplifier in the forward–pumping

The following fundamental properties of SRS are critical for designing Raman fiber amplifiers [12]:

1) Raman gain has a spectral shape that depends primarily on the frequency *separation* between a pump and signal, not their absolute frequencies. This follows from energy conservation: their frequency separation must equal the frequency of the optical phonon that is created.
2) Raman gain does not depend on the relative direction of propagation of a pump and signal. The optical branch of the phonon $\omega - k$ diagram is quite flat, and so phonons of a given frequency exist with a broad range of momenta or k-vectors. Therefore, momentum conservation is guaranteed irrespective of the relative directions of pump and signal photons.
3) Raman scattering is a fast process (subpicosecond). Because SRS is nonresonant (i.e., the upper state is virtual), there are no long upper-state lifetimes to buffer pump

fluctuations as there are, for example, in EDFAs. However, for reasons of efficiency, Raman amplifiers typically consist several kilometers of fiber. Then, a given portion of signal light can pass through many pump fluctuations if the signal and pump propagate in opposite directions, or if they copropagate at different velocities. This averaging effect can reduce the impact of pump fluctuations.

4) Raman gain is polarization dependent. The peak coupling strength between a pump and signal is approximately an order of magnitude stronger if they are co polarized than if they are orthogonally polarized.

Raman amplifiers are called lumped or distributed depending on their design. In the case of distributed Raman amplification, the same fiber that is used for signal transmission is also used for signal amplification.

2.3 Scaling of Raman gain coefficient

The Raman-gain coefficient g_R is related to the optical gain, the ratio g_R / A_{eff} is a measure of the Raman-gain efficiency [2].

Figure 2.3 shows the measurements of g_R / A_{eff} (C_R) for three types of Germanosilicate fibers with different 1550-nm effective areas: a dispersion compensating fiber (DCF $15 um^2$), a nonzero dispersion fiber (NZDF, $55 um^2$), and a superlarge effective area fiber (SLA, $105 um^2$). For each case the pump wavelength was 1450 nm, and g_R / A_{eff} is plotted versus the frequency difference between the pump and signal. The Raman gain efficiency spectra are all roughly triangular in shape, peaking at approximate 13 to 14 THz. These peaks are broader than those of crystalline materials, because there a continuum of molecular vibrational frequencies due to the amorphous nature of silica-based glass [12].

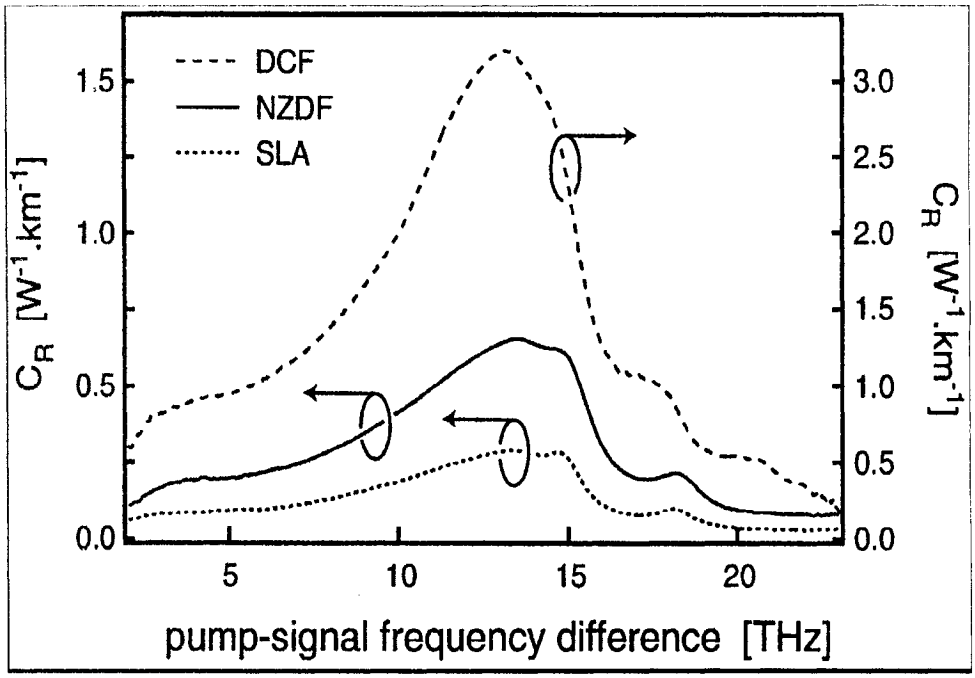

Figure 2.3 Raman-gain efficiency spectra of three types of Germanosilicate fibers, for a pump wavelength of 1450 nm.

However, the peak values of these g_R / A_{eff} spectra are clearly different. These peak values depend on the effective areas and degree of overlap of the pump and signal transverse modes, and are *approximately* inversely proportional to the effective area of the signal mode. Differences also result from compositional distinctions between the fibers. In addition, for a given fiber, the maximum value of g_R / A_{eff} (C_R) depends on the specific pump wavelength, typically increasing as the pump wavelength is reduced [2].

In [14], the relations between g_R, A_{eff}, and pump wavelength are clearly illustrated as in Eq 2.1.

$$g_R(\Delta\nu, \Lambda_p) = g_R(\Delta\nu, \lambda_p) \times \frac{\lambda_s}{\Lambda_s} \times \left[\frac{A_{eff-ps}(\Delta\nu, \lambda_p)}{A_{eff-ps}(\Delta\nu, \Lambda_p)} \right] \tag{2.1}$$

where $$A_{eff-ps}(\Delta\nu, \lambda_p) = \frac{1}{2} \times \left[A_{eff}(\lambda_p) + A_{eff}(\lambda_s) \right]$$

$\Delta\nu$ is the frequency separation between pump and signal; Λ_p, Λ_s, λ_p, and λ_s

represent new pump, signal wavelength, and reference pump, signal wavelength respectively; and relative effective fiber area between a pump and a signal is represented by $A_{eff-ps}(\Delta v, \lambda_p)$.

Next, an example is given for application of this equation.

- How to find the g_R value of one signal (wavelength = 1555 nm) pumped by one pump located at 1425 nm. Fiber type is TW-Reach fiber.
- Known information: Reference g_R spectrum given by the reference wavelength of 1460 nm (see Figure 2.4), and TW-Reach fiber A_{eff} data at any wavelengths.
- Solution:

  Step 1:

  Calculate the frequency separation between the signal (1555 nm) and the new pump (1425 nm) with equation of $\Delta v = \frac{C}{\lambda_p} - \frac{C}{\lambda_s}$. Here, $\lambda_p = 1425nm$, and $\lambda_s = 1555nm$. C is light speed ($C = 2.99792458 \times 10^8 m/s$). Then, we obtain $\Delta v = 16977.9GHz$.

  Step 2:

  Find out g_R value based on $\Delta v = 16977.9GHz$ in the referenced Raman gain coefficient spectra ($g_R(\Delta v, \lambda_p) = 0.17219(W \cdot km)^{-1}$), and the reference signal wavelength λ_s with $\lambda_s = \frac{C}{\frac{C}{\lambda_p} - \Delta v}$, where, λ_p is the reference pump wavelength ($\lambda_p = 1460nm$). Therefore, we obtain $\lambda_s = 1591nm$.

  Step 3:

  Finding A_{eff} values in A_{eff} data file at wavelengths: $\lambda_p = 1460nm$,

$\lambda_s = 1591nm$, and new pump and signal wavelengths: $\Lambda_p = 1425nm$, $\Lambda_s = 1555nm$, then we calculated $A_{eff-ps}(\Delta v, \lambda_p)$ and $A_{eff-ps}(\Delta v, \Lambda_p)$ with equation of $A_{eff-ps}(\Delta v, \lambda_p) = \frac{1}{2} \times [A_{eff}(\lambda_p) + A_{eff}(\lambda_s)]$. From A_{eff} data file, we know the following:

$$A_{eff}(\lambda_p = 1460\,nm) = 47.50461397\,\mu m^2$$
$$A_{eff}(\lambda_s = 1591\,nm) = 57.74642775\,\mu m^2$$
$$A_{eff}(\Lambda_p = 1425\,nm) = 46.22804304\,\mu m^2$$
$$A_{eff}(\Lambda_s = 1555\,nm) = 54.73575389\,\mu m^2$$

Calculated results are:

$$A_{eff-ps}(\Delta v, \lambda_p) = 52.62552086\,\mu m^2$$
$$A_{eff-ps}(\Delta v, \Lambda_p) = 50.48189797\,\mu m$$

Step 4:

Finally, using Equation (2.1) to get g_R expected and $g_R = 0.183657(W \cdot km)^{-1}$.

Figure 2.4 shows comparison for TW-RS fiber in [14] between calculations by Eq. 2.1 and measurements. To confirm the correctness of g_R scaling in this thesis, our calculations for TW-Reach fiber are shown in Figure 2.5. It is clearly shown that the g_R scaling trends in Figure 2.4 and Figure 2.5 are the same, which proves that our calculations are correct.

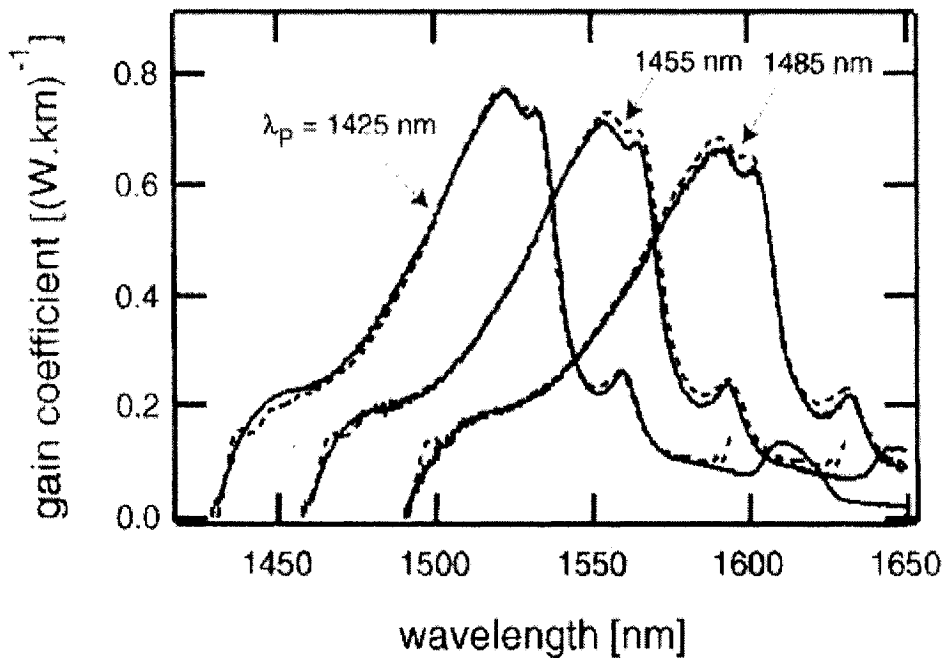

Figure 2.4 Predicted (dashed curves) and measured (solid curves) Raman gain spectra on a TrueWave RS fiber from [14].

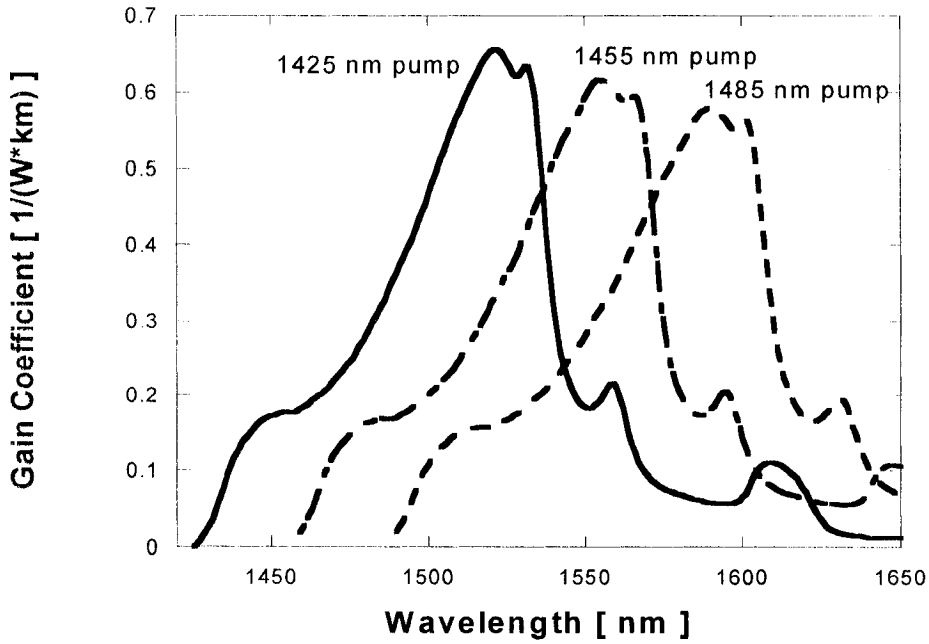

Figure 2.5 Raman gain coefficient scaling for TW-Reach fiber.

Solid curve is for 1425 nm pump. Dot-dash curve is for 1455 nm pump; dot curve is for 1485 nm pump.

CHAPTER 3 Fiber Raman Amplifier Model

Raman gain has a spectral shape that depends primarily on the frequency separation between a pump and signal, not their absolute frequencies. The spectral flexibility of Raman amplification allows the gain spectrum to be shaped by combining multiple pump wavelengths to make a polychromatic pump spectrum. Therefore, fiber Raman amplifiers have been considered as a flexible and simple way to amplify signal in both C and L band. Accordingly, the accuracy of fiber Raman amplifier modeling becomes extremely important, and many scientists have made their contributions in establishing and improving it. Stolen et al. described modeling of Stokes amplified spontaneous emission (ASE) and multiple Stokes shifts in single-mode fiber. Kidorf et al. gave detailed equations for a Raman amplifier model applied to single-mode optical fiber. Achtenhagen et al. verified the gain predicted by this model, added Rayleigh backscattering and wavelength scaling approximation to account for effective fiber core area. Perlin et al. added anti-Stokes spontaneous emissions. Berntson et al. corrected the equation given by Kidorf in for spontaneous absorption of signal photons [15].

In this thesis, we use the Raman amplifier model for single-model fiber given in [15], which for the first time, explicitly gives the Raman propagation equation in both coconfiguration and counterconfiguration, and includes effects due to group velocity, Rayleigh backscattering fiber loss as well as stokes and anti-stokes spontaneous emission [15].

This chapter contains some contents from Ting Zhang's master thesis, as we share the same fiber Raman amplifier modeling and simulation solution.

3.1 Basic definitions

Figure 3.1 shows a general fiber Raman amplifier.

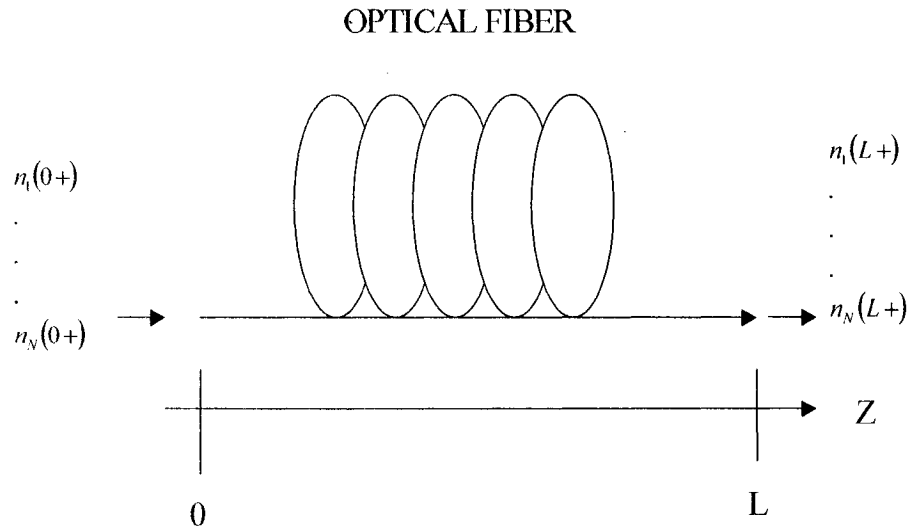

Figure 3.1 General Raman amplifiers.

$n_1(0+)..n_N(0+)$ are the numbers of photons in the forward traveling signal and pump beams at the input. Correspondingly, $n_1(L+)..n_N(L+)$ are the numbers of photons in the forward traveling ones at the output. L is the length of the optical fiber and z is the position in the fiber.

Parameters used to characterize the optical fiber are: length L; frequency dependent fiber attenuation $\alpha(v)$; Raman gain coefficient $g_R(\Delta v, \lambda_p)$, which depends on the frequency separation between beams, and the shorter wavelength between two channels; frequency dependent Rayleigh scattering coefficient $\gamma(v)$ and effective area of the fiber $A_{eff}(v)$; and absolute temperature T of the optical fiber. For the position reference, z is used, which is set to zero at the input end, and L at the output end. Signal and pump beams having photon numbers of n_i traveling in the forward and backward direction are written as n_i^+, n_i^-, respectively. Therefore, $n_i(0+)$ is the input, and $n_i(L+)$ is the output. If the pump beam is injected backwardly, it is denoted as $n_i(L-)$. Otherwise, it is included in the input side.

We use P_i to express the beam power for channel i in a limited bandwidth. This channel i can be signal or pump, and P_i is defined in Eq. 3.1, where v_i is the frequency of the i-th channel. ASE noise power is calculated in a bandwidth of Δv. To indicate the difference, ASE noise power is denoted by P_i^{ASE}, and the definition is in Eq. 3.2. Eq. 3.3 is the relationship between Raman gain and Raman gain coefficient g_R.

$$P_i = h v_i n_i \tag{3.1}$$

$$P_i^{ASE} = \int_{\Delta v_i} n(v) h v dv \tag{3.2}$$

$$G(v_{signal}, v_{pump}) = g_R(v_{signal}, v_{pump}) \times P_{pump} \tag{3.3}$$

Raman gain is to indicate the amplification degree. The absolute gain from position z_1 to z_2 is defined in Eq. 3.4, as P_s is the signal power at the two positions.

$$G_{absolute}(z_1 \rightarrow z_2) = \frac{P_s(z_2)}{P_s(z_1)} \tag{3.4}$$

The on-off Raman gain from position z_1 to z_2 is defined in Eq. 3.5, which is the absolute gain minus fiber loss. Here α is in dB/km, and $L = z_1 - z_2$ is in km.

$$G_{on-off}(z_1 \rightarrow z_2)[dB] = G_{absolute}(z_1 \rightarrow z_2)[dB] - \alpha L \tag{3.5}$$

The noise figure of a Raman amplifier describes the noise performance, and it is defined by Eq. 3.6 [15]. If the G is the on-off gain, the resulting noise figure is called equivalent noise figure (ENF).

$$F = \frac{1}{G}\left[\frac{P^{ASE+}(L)}{h v \Delta v} + 1\right] \tag{3.6}$$

where $P^{ASE+}(L)$ is the forward ASE noise power in bandwidth of Δv at the output end.

3.2 General model

Eq. 3.7 is our base of Raman amplifier model given in [15] by Stokes and anti-Stokes analysis.

$$\pm\frac{dP_i^{\pm}}{dz} = -\alpha(v_i,T)P_i^{\pm} \quad ①$$

$$+\gamma(v_i)P_i^{\mp} \quad ②$$

$$+P_i^{\pm}\sum_{j}^{v_j>v_i} g_R(v_j,v_i)\left[P_j^{+}+P_j^{-}\right] \quad ③$$

$$+2\sum_{j}^{v_j>v_i}\left[P_j^{+}+P_j^{-}\right]hv_i\Delta v g_R(v_j,v_i)\times\left(1+\frac{1}{e^{\frac{h(v_j-v_i)}{kT}}-1}\right) \quad ④$$

$$-P_i^{\pm}\sum_{j}^{v_j<v_i}\frac{V_j}{V_i}\frac{v_j}{v_i}g_R(v_i,v_j)\left[P_j^{+}+P_j^{-}\right] \quad ⑤$$

$$+2\sum_{j}^{v_j<v_i}\left[P_j^{+}+P_j^{-}\right]hv_i\Delta v\frac{v_j}{v_i}\frac{V_j}{V_i}\times g_R(v_i,v_j)\frac{1}{e^{\frac{h(v_i-v_j)}{kT}}-1} \quad ⑥$$

(3.7)

Where h is Planck's constant, k is the Boltzmann constant, T is the temperature, v_j and v_i are the frequencies, V_i or V_j is group velocity denoted by subscript for different frequencies, and P_i^{+} and P_i^{-} are the power at the i-th frequency in forward and backward, respectively.

In Eq. 3.7, portion ① and ② represent fiber loss and Rayleigh scattering; portion ③ is the gain from higher frequencies and ⑤ is the depletion to lower frequencies; ④ and ⑥ are noise due to stimulated spontaneous emission, and anti-Stokes, respectively.

To apply this differential format equation to a fiber Raman amplifier with length L, the fiber can be equally separated into m segments, each with a length of $\Delta z = \frac{L}{m}$ as shown in Figure 3.2.

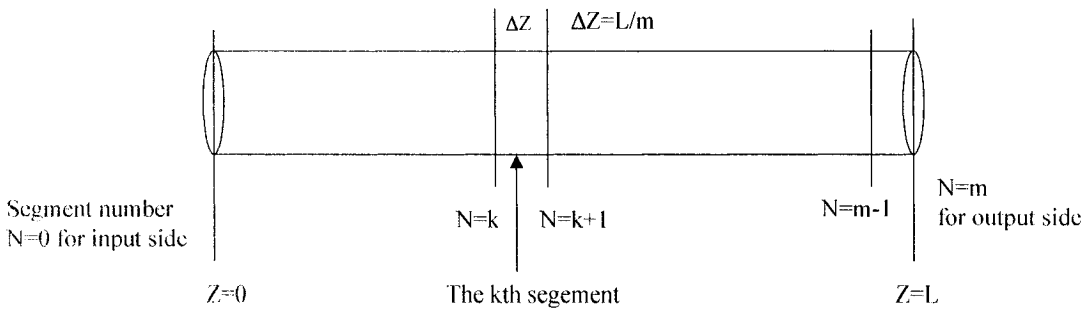

Figure 3.2 Transmission-fiber is separated into m segments to apply the integration in propagation equation.

Then, Eq. 3.7 can be written into Eq. 3.8.

$$\frac{dP_i^+(z_{k+1})}{dz} = -\alpha(v_i)P_i^+(z_k) + \gamma(v_i)P_i^-(z_k)$$

$$+ P_i^+(z_k)\sum_j^{v_j>v_i} g_R(v_j,v_i)\left[P_j^+(z_k)+P_j^-(z_k)\right]$$

$$+ 2\sum_j^{v_j>v_i}\left[P_j^+(z_k)+P_j^-(z_k)\right]hv_i\Delta v g_R(v_j,v_i)\times\left(1+\frac{1}{\exp\left(\frac{h(v_j-v_i)}{kT}\right)-1}\right)$$

$$- P_i^+(z_k)\sum_j^{v_j<v_i}\frac{V_j}{V_i}\frac{v_j}{v_i}g_R(v_i,v_j)\left[P_j^+(z_k)+P_j^-(z_k)\right]$$

$$+ 2\sum_j^{v_j<v_i}\left[P_j^+(z_k)+P_j^-(z_k)\right]hv_i\Delta v\frac{v_j}{v_i}\frac{V_j}{V_i}\times g_R(v_i,v_j)\left(\frac{1}{\exp\left(\frac{h(v_i-v_j)}{kT}\right)-1}\right)$$

(3.8a)

$$\frac{dP_i^-(z_k)}{dz} = -\alpha(v_i)P_i^-(z_{k+1}) + \gamma(v_i)P_i^-(z_{k+1})$$

$$+P_i^-(z_{k+1})\sum_j^{v_j>v_i} g_R(v_j,v_i)\left[P_j^+(z_{k+1})+P_j^-(z_{k+1})\right]$$

$$+2\sum_j^{v_j>v_i}\left[P_j^+(z_{k+1})+P_j^-(z_{k+1})\right]hv_i\Delta v g_R(v_j,v_i)\times\left(1+\frac{1}{\exp\left(\frac{h(v_j-v_i)}{kT}\right)-1}\right)$$

$$-P_i^-(z_{k+1})\sum_j^{v_j<v_i}\frac{V_j}{V_i}\frac{v_j}{v_i}g_R(v_i,v_j)\left[P_j^+(z_{k+1})+P_j^-(z_{k+1})\right]$$

$$+2\sum_j^{v_j<v_i}\left[P_j^+(z_{k+1})+P_j^-(z_{k+1})\right]hv_i\Delta v\frac{v_j}{v_i}\frac{V_j}{V_i}\times g_R(v_i,v_j)\left(\frac{1}{\exp\left(\frac{h(v_i-v_j)}{kT}\right)-1}\right)$$

(3.8b)

Here, z_k is the k-th segment ($0 \le k \le m$). So, $P_i^+(z_0)$ is input signal and forward pump power, and $P_i^+(z_m)$ is the output. If the Raman amplifier is backward pumped, using $P_i^-(z_m)$ to indicate the inputted pump power.

3.3 Equations for signals, pumps, and ASE noise

From Eq. 3.7 and Eq. 3.8, we can separate the signal portion and noise portion, and write them as in Eq. 3.9, Eq. 3.10 and Eq. 3.11.

Signal equations:

Forward:

$$\frac{dP_i^+(z_{k+1})}{dz}=-\alpha(v_i)P_i^+(z_k)$$

$$+P_i^+(z_k)\sum_{j}^{v_j(pumps+signals)>v_i} g_R(v_j,v_i)\left[P_j^+(z_k)+P_j^-(z_k)\right]$$

$$-P_i^+(z_k)\sum_{j}^{v_j(signals+noise)<v_i} \frac{V_j}{V_i}\frac{v_j}{v_i} g_R(v_i,v_j)\left[P_j^+(z_k)+P_j^-(z_k)\right]$$

(3.9)

Pump equations:

Forward:

$$\frac{dP_i^+(z_{k+1})}{dz} = -\alpha(v_i)P_i^+(z_k)+\gamma(v_i)P_i^-(z_k)$$

$$+P_i^+(z_k)\sum_{j}^{v_j(pumps)>v_i} g_R(v_j,v_i)\left[P_j^+(z_k)+P_j^-(z_k)\right]$$

$$-P_i^+(z_k)\sum_{j}^{v_j(pumps+signals+noise)<v_i} \frac{V_j}{V_i}\frac{v_j}{v_i} g_R(v_j,v_i)\left[P_j^+(z_k)+P_j^-(z_k)\right]$$

(3.10a)

Backward:

$$\frac{dP_i^-(z_k)}{dz} = -\alpha(v_i)P_i^-(z_{k+1})+\gamma(v_i)P_i^+(z_{k+1})$$

$$+P_i^-(z_{k+1})\sum_{j}^{v_j(pumps)>v_i} g_R(v_j,v_i)\left[P_j^+(z_{k+1})+P_j^-(z_{k+1})\right]$$

$$-P_i^-(z_{k+1})\sum_{j}^{v_j(pumps+noise)<v_i} \frac{V_j}{V_i}\frac{v_j}{v_i} g_R(v_j,v_i)\left[P_j^+(z_{k+1})+P_j^-(z_{k+1})\right]$$

(3.10b)

ASE noise power:

Forward:

$$\frac{dP_i^+(z_{k+1})}{dz} = -\alpha(v_i)P_i^+(z_k)+\gamma(v_i)P_i^-(z_k)$$

$$+P_i^+(z_k)\sum_{j}^{v_j>v_i} g_R(v_j,v_i)\left[P_j^+(z_k)+P_j^-(z_k)\right]$$

$$+2hv_i\Delta v\sum_j^{v_j>v_i} g_R(v_j,v_i)\left[P_j^+(z_k)+P_j^-(z_k)\right]\left[1+\frac{1}{\exp\left(\frac{h(v_j-v_i)}{kT}\right)-1}\right]$$

$$-P_i^+(z_k)\sum_j^{v_j<v_i}\frac{V_j}{V_i}\frac{v_j}{v_i}g_R(v_j,v_i)\left[P_j^+(z_k)+P_j^-(z_k)\right]$$

$$+2hv_i\Delta v\sum_j^{v_j<v_i}\frac{V_j}{V_i}\frac{v_j}{v_i}g_R(v_j,v_i)\left[P_j^+(z_k)+P_j^-(z_k)\right]\left[\frac{1}{\exp\left(\frac{h(v_i-v_j)}{kT}\right)-1}\right]$$

(3.11a)

Backward:

$$\frac{dP_i^-(z_k)}{dz}=-\alpha(v_i)P_i^-(z_{k+1})+\gamma(v_i)P_i^+(z_{k+1})$$

$$+P_i^-(z_{k+1})\sum_j^{v_j>v_i}g_R(v_j,v_i)\left[P_j^+(z_{k+1})+P_j^-(z_{k+1})\right]$$

$$+2hv_i\Delta v\sum_j^{v_j>v_i}g_R(v_j,v_i)\left[P_j^+(z_{k+1})+P_j^-(z_{k+1})\right]\left[1+\frac{1}{\exp\left(\frac{h(v_j-v_i)}{kT}\right)-1}\right]$$

$$-P_i^-(z_{k+1})\sum_j^{v_j<v_i}\frac{V_j}{V_i}\frac{v_j}{v_i}g_R(v_j,v_i)\left[P_j^+(z_{k+1})+P_j^-(z_{k+1})\right]$$

$$+2hv_i\Delta v\sum_j^{v_j<v_i}\frac{V_j}{V_i}\frac{v_j}{v_i}g_R(v_j,v_i)\left[P_j^+(z_{k+1})+P_j^-(z_{k+1})\right]\left[\frac{1}{\exp\left(\frac{h(v_i-v_j)}{kT}\right)-1}\right]$$

(3.11b)

3.4 Raman amplifier model verification: Raman gain and ASE noise

To prove the accuracy of our modeling, we verify it with the experimental results in [15]. Following are two verification vases.

3.4.1 Verification case 1

Case 1 is based on an 80-km single mode fiber at 300 K temperature. The input is a 0.001mW signal at 1543 nm. Comparison results are shown in Figure 3.3. Our result is in good match in shape with the result from [15]. The difference on the absolute value is due to different fiber parameters used.

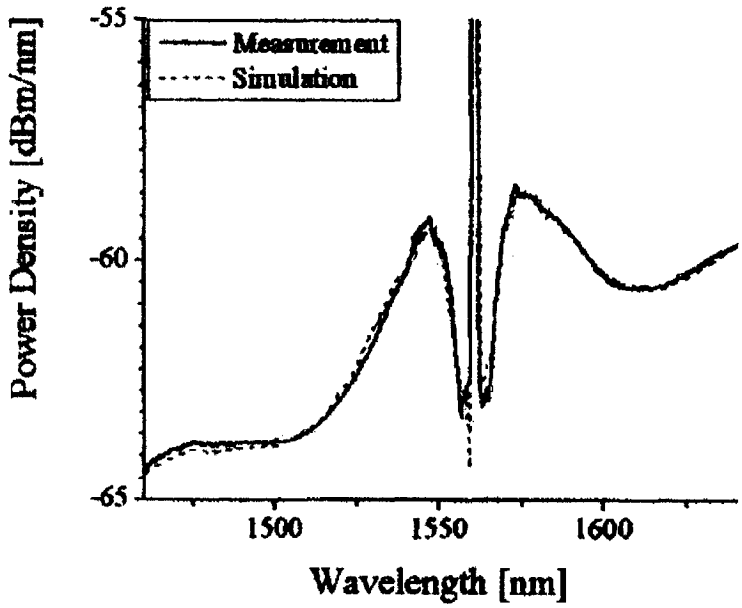

(a)

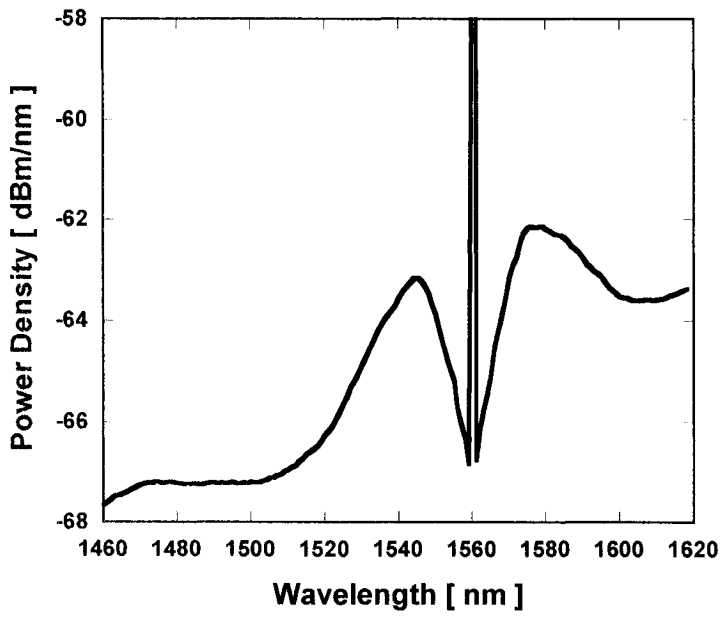

(b)

Figure 3.3 Verification 1, (a) from [15] and (b) from our modeling

3.4.2 Verification case 2

Case 2 is based on 100 km Corning SMF-28 fiber, with 51 C band signals. The channel spacing is 100 GHz and each input channel has a power of 1.96 mW. Two pumps, 300 mW at 1430 nm and 262.5 mW at 1454 nm are implied. Figure 3.4 shows the comparison results on on-off gain.

Gain spectrums in Figure 3.4 are in good match. The difference in absolute gain values is due to different fiber parameters used.

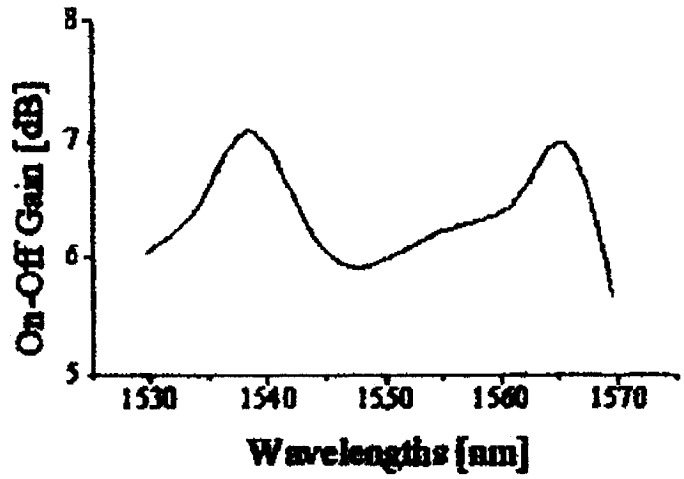

(a)

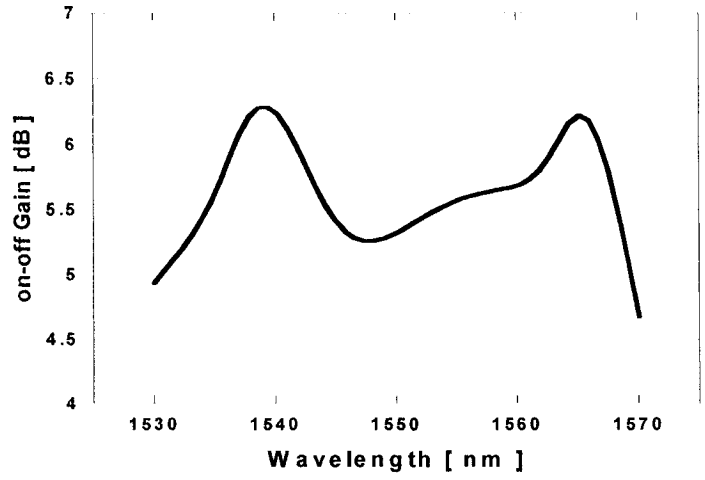

(b)

Figure 3.4 Verification 2, (a) from [15] and (b) from our work

The verifications above confirm the accuracy of our modeling.

3.5 MPI noise

In evaluating FRA noise performance, two main contributions are to be taken into account: ASE and Rayleigh backscattering impact [11]. Rayleigh scattering is the source of two noise contributions: one due to Rayleigh scattering of the ASE counter propagating with respect to the signal and the second due to double Rayleigh scattering (DRS) of the signal [16]. Signal DRS originates an incoherent multiple path interference

(MPI), which is a noise generated by the beating of multiple differently delayed replicas of the signal itself [11]. We have verified ASE noise simulation in Section 3.4. In this section, we will explain MPI noise and verify our modeling with the experimental results from published papers.

Rayleigh scattering can occur in an optical fiber due to small inhomogeneities [4, 5, and 12] or microscopic variations in the refractive index. Portion of the signal is backscattered by Rayleigh scattering process and it suffers the gain, supplied by Raman pumping, more than twice before it is combined with the signal. Because of their long lengths and their nonuniform gain distribution, fiber Raman amplifiers (FRA) are more likely to suffer from generation of DRB. Noise due to DRS of the signal in the gain fiber is one of the most significant limiting factors in the design of a Raman amplifier.

Figure 3.5 is the experimental setup in [11], we will use this setup to prove the accuracy of our Raman amplifier model. Two verification cases are investigated.

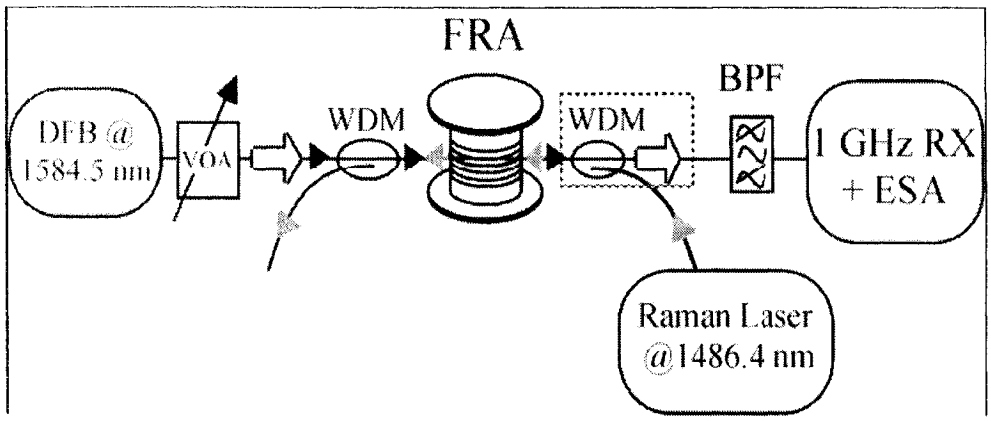

Figure 3.5 Experimental setup in [11]

3.5.1 Verification case 1

Case one is based on a SMF distributed fiber Raman amplifier. The parameters used are listed in the following table.

Table 3.1: Verification case 1 parameters

fiber length	80 km
Rayleigh backscattering coefficient K_{RS}	-40 dB/km
fiber attenuation at pump wavelength α_P	0.2 dB/km
fiber attenuation at signal wavelength α_S	0.2 dB/km
Raman gain coefficient C_R	$3x10^{-4}$ ($m^{-1}W^{-1}$)
input signal power $P_s(0)$	-30 dBm
pump power P_{pump}	100 to 2000 mW

The comparison results are shown in Figure 3.6. Our simulation results are in good match with those results from [11] and [17], [18].

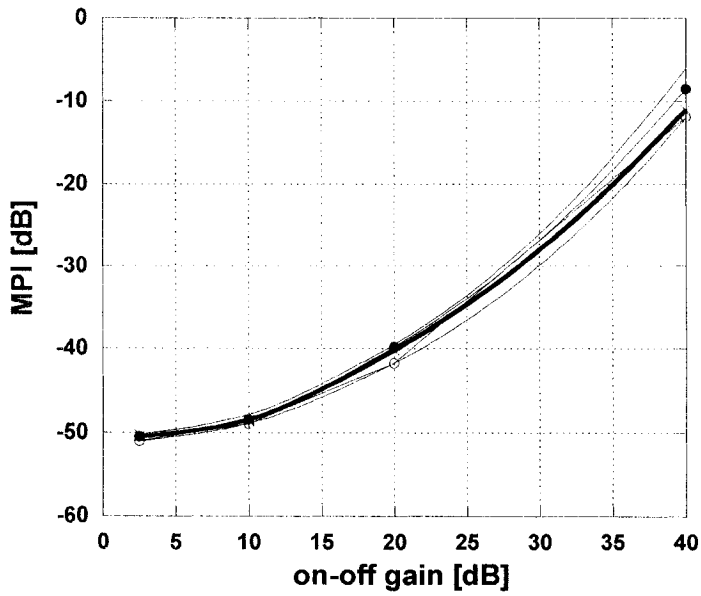

Figure 3.6 Case 1 comparison results.

Black circle: results from [10]; blank circle: results from [18];

Star: Results from [17]; Solid: our simulation results.

3.5.2 Verification case 2

Case two is based on a LRA. The parameters used are listed in the following table.

Table 3.2: Verification case 2 parameters

fiber length	12 km
Rayleigh backscattering coefficient K_{RS}	-40 dB/km
fiber attenuation at pump wavelength α_P	0.2 dB/km
fiber attenuation at signal wavelength α_S	0.2 dB/km
Raman gain coefficient C_R	$7x10^{-4}$ ($m^{-1}W^{-1}$)
input signal power $P_s(0)$	-30 dBm
pump power P_{pump}	100 to 2000 mW

The comparison results are shown in Figure 3.7. Our simulation results are also in good match with those results from [11] and [17], [18].

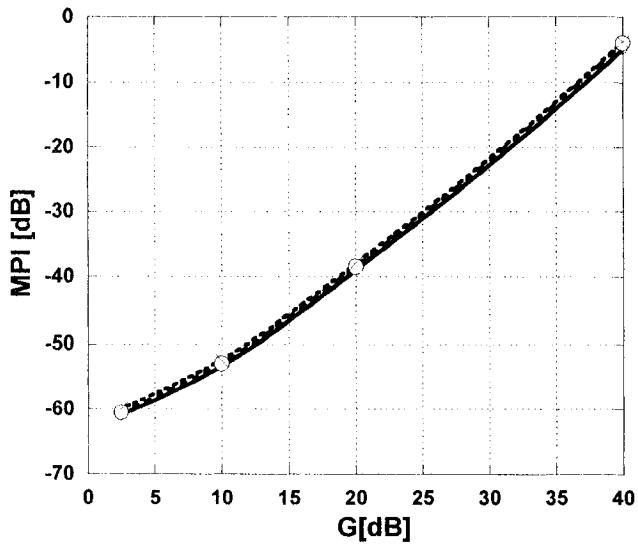

Figure 3.7 Case 2 comparison results.

Star: Result from [11]; blank circle: result from [17] [18].

Solid: our simulation results.

CHAPTER 4 Fiber Parameters for FRAs

Fibers from different manufactures or even the same manufacture may have different parameter values. In this chapter, we will introduce the fibers used in our simulations, their parameters will be described and values will be given.

4.1 Dispersion Compensating Fiber (DCF)

DCF was invented originally to compensate the fiber dispersion and/or dispersion slope in the transmission fiber. However, it was found out that DCF is an excellent gain medium for discrete Raman amplifiers. The discrete Raman amplification only requires a few kilometers of fiber. In addition, the small effective area and high *Ge* concentration of DCF provide high Raman gain efficiency. What's more, the DCF as a discrete Raman amplifier can give additional flexibility in the system; it can save more space in the practical application. For these reasons, LRA with DCF is becoming more and more widely used in the long-haul and ultra-long haul transmission system.

The DCF we used for our simulations has the following parameters listed in Table 4.1. Those values are experimental results and widely used in published papers.

Table 4.1 DCF fiber parameters

Parameter	Unit	Value
Fiber attenuation @ 1200 nm	dB/km	1.15
@ 1450 nm		0.54
@ 1550 nm		0.41
@ 1700 nm		0.54
Cutoff wavelength	nm	1400
Dispersion at 1550 nm	ps/km/nm	-93
γ	1/W/km	12.0

g_R / A_{eff}	1/W/km	2.46

4.2 Highly Nonlinear Fiber (HNLF)

HNLF is a fiber with high non-linearity to generate Raman gain efficiently and used as a gain medium for the lumped Raman amplifier. With HNLF, high gain can be obtained with much shorter length of the fiber and it can be packed into a compact package. By employing the HNLF, it's possible to construct the LRA with high conversion efficiency [19].

Total Raman Gain (G_R) can be calculated by the equation below, low attenuation is quite important for Raman Gain as well as Raman Gain Coefficient [19].

$$G_R\ [dB]=10\ \log[\exp(\frac{g_R}{A_{eff}} P_p\ L_{eff})$$

where g_R/A_{eff} : Raman gain coefficient intrinsic to fiber characteristics

P_p : Pump power inputted into the fiber

L_{eff} : Effective length for pumping light

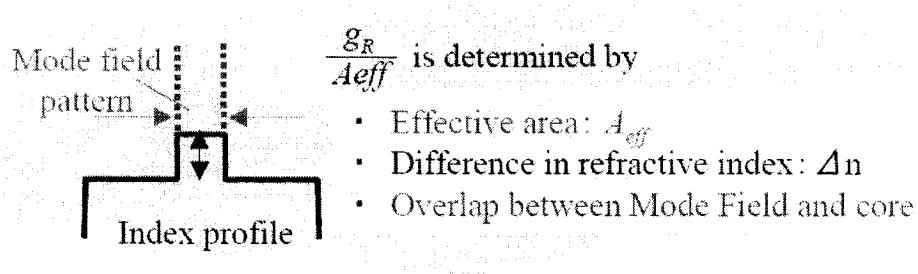

Figure 4.1 HNLF fiber structure

The HNLF fiber used in our simulation is commercially available on the market from Sumitomo Electric Industries Ltd. Its parameters are listed in the following table.

Table 4.2 HNLF fiber parameters

Parameter		Unit	Value
Fiber attenuation	@ 1200 nm	dB/km	1
	@ 1450 nm		0.61
	@ 1550 nm		0.46
	@ 1700 nm		0.52
Cutoff wavelength		nm	1400
Dispersion at 1550 nm		ps/km/nm	-13.6
γ		1/W/km	23.6
g_R / A_{eff}		1/W/km	7.2

As for the Rayleigh scattering coefficient, it's not published on any documents. We will determine its value in the following way.

Rayleigh scattering coefficient plays an important role in fiber attenuation. The losses occurring in silica glass fibers can be classified as Rayleigh scattering, imperfection loss and other components as shown in Eq. 4.1. Where A is the Rayleigh scattering coefficient, B is imperfection loss and C is a function of wavelength λ such as infrared absorption loss, bending loss, and OH absorption loss. Rayleigh scattering, which is inversely proportional to the fourth power of wavelength, is caused by variations in the density of the glass and also induced by doping of germanium [11].

$$\alpha = \frac{A}{\lambda^4} + B + C(\lambda) \tag{4.1}$$

We repeated the experimental setup in [3] to get the Rayleigh scattering coefficient value by simulation. 3km HNLF is used in the 4-channel CWDM system experimental setup shown below. The HNLF-based LRA provide a net gain of 10-dB for 4-channel CWDM signals, which has the output signal power of 10dBm/ch.

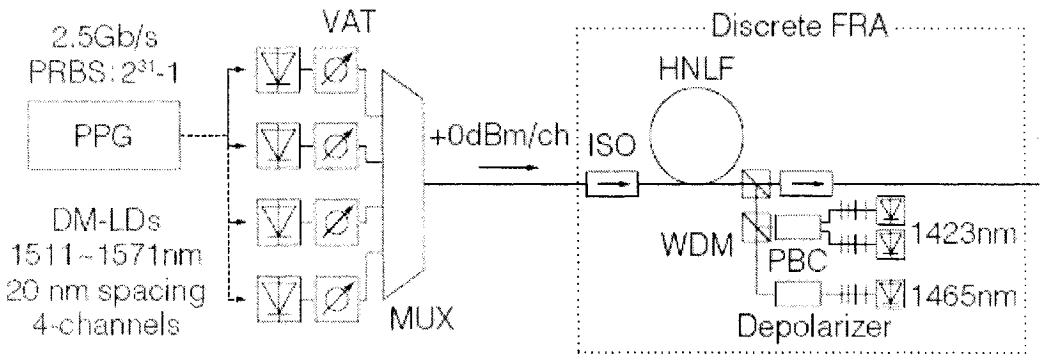

Figure 4.2 Experimental setup in [3].

The wavelengths of 4-channel CWDM signals from multi-quantum well (MQW) DM-LDs were arranged from 1511 nm to 1571 nm with 20 nm spacings. The bit rate of each CWDM signal was 2.5 Gb/s. To flatten the net gain over the 60 nm bandwidth and to construct a simple FRA, only two pump wavelengths from fiber grating lasers have been set to be 1423 nm and 1465 nm.

A total pumping power of 415 mW was employed, and the experimental results are shown in the following table.

Table 4.3 Experimental results from [3]

Net gain [dB]	10
Gain ripple [dB]	1.5
Noise figure [dB]	5.8

Suppose different value of Rayleigh scattering coefficient R, we get the following results.

(i) R= -35.85 dB/km @1550 nm

Table 4.4 Case R= -35.85 dB/km

Average net gain [dB]	10.67
Gain ripple [dB]	0.83

Noise figure [dB]	5.6

(ii) R= -34.69 dB/km @1550 nm

Table 4.5 Case R= -34.69 dB/km

Average net gain [dB]	10.68
Gain ripple [dB]	0.83
Noise figure [dB]	7.2

Our simulation results on amplifier gain match the experimental results. For the Rayleigh scattering coefficient, its value is proved to be within the range of -35.85 dB/km and -34.69 dB/km.

The Rayleigh scattering coefficient degrades the amplifier's noise performance, but doesn't affect gain performance. We will compare LRAs with HNLF and LRAs with DCF in our thesis, and use the same Rayleigh scattering coefficient value as DCF in this paper unless otherwise stated.

In Appendix A, you will find the fiber parameters used in this thesis.

CHAPTER 5 Performance of LRAs with Single Pump

In this chapter, we will investigate LRAs with different amplification medium pumped by single pump. Section 5.1 gives the description of our simulation cases. Section 5.2 demonstrates eight simulation cases and along with the simulation results. Conclusions and more discussions are given in Section 5.3.

5.1 Setup of simulation cases

The aim of this chapter is to compare the Raman gain and the noise characteristics performance between LRAs with DCF and LRAs with HNLF as Raman gain medium from a normal application: small signals in C band amplified by LRA. 100 C band signals are chosen. It's found that 1453 nm is the optimized pump wavelength to achieve flat gain over C band. The common setups of these simulation cases are summarized in the following table.

Table 5.1 Common setups of simulation cases

Input signal power	0.01 mW (-20 dBm) /Ch
Signal bandwidth	1530 – 1570 nm
Signal channel spacing	50 GHz
Number of channels	100
Pump wavelength	1453 nm
Pump power	100-1000 mW

We will investigate different simulation cases to compare the Raman gain, the OSNR and the noise figure performance between LRAs with HNLF and LRAs with DCF. We also found that with the above settings, channel 1552.18nm has the worst OSNR value among all channels, i.e., channel 1552.18nm has the worst noise performance. For the whole transmission system, the worst performance channel is the bottleneck for system

noise character. So it is safe for us to choose channel 1552.18 nm for noise performance comparisons. All the following results shown are data of channel 1552.18 nm unless otherwise stated.

The following table summarizes all simulation cases in this chapter.

Table 5.2 Simulation cases summary

1	Comparisons between LRAs with 3000m DCF or HNLF as gain medium
2	Comparisons between LRAs with 900m or 3000m HNLF as gain medium
3	Comparisons between LRAs with 3000m or 8000m DCF as gain medium
4	Comparisons between LRAs with DCF or HNLF, fixed pump power 300mW
5	Comparisons between LRAs with DCF or HNLF, fixed pump power 400mW
6	Comparisons between LRAs with DCF or HNLF, fixed amplifier gain 15 dB
7	Comparisons between LRAs with DCF or HNLF, whole C band
8	Comparisons between different pumping schemes

5.2 Simulation cases and results

5.2.1 Comparisons between LRAs with 3000m DCF or HNLF as a gain medium

First, we want to have an idea how efficiently HNLF can work as a Raman gain medium. We choose 3000m fiber as the gain medium to compare the Raman gain efficiency between HNLF and DCF. The LRAs are counter pumped and the simulation results are shown in Figure 5.1.

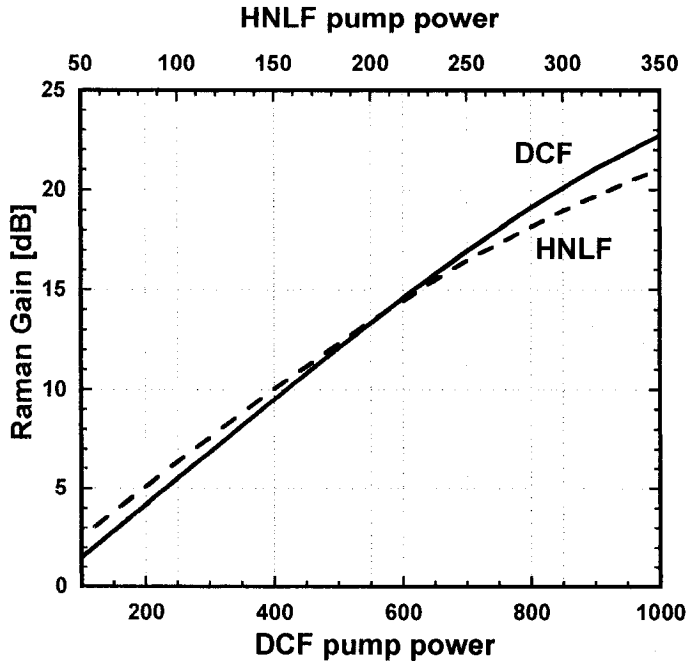
HNLF pump power
50
100
150
200
250
300
350
25
20
15
10
5
0
Raman Gain [dB]
DCF
HNLF
200
400
600
800
1000
DCF pump power

(a)

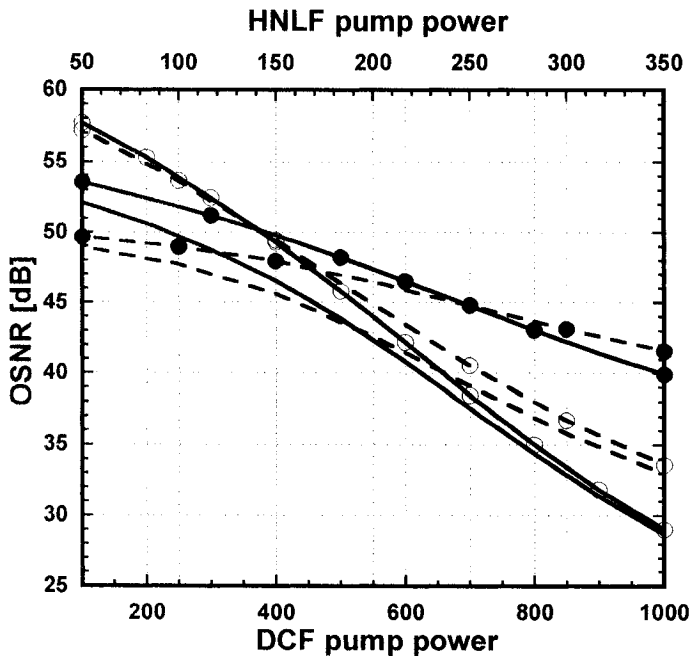
HNLF pump power
50
100
150
200
250
300
350
60
55
50
45
40
35
30
25
OSNR [dB]
200
400
600
800
1000
DCF pump power

(b)

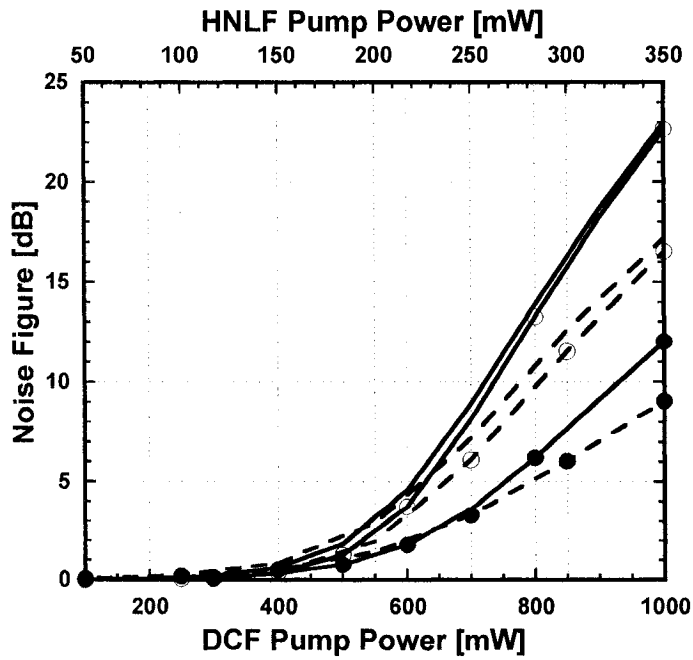
HNLF Pump Power [mW]
50
100
150
200
250
300
350
25
20
15
10
5
0
Noise Figure [dB]
200
400
600
800
1000
DCF Pump Power [mW]

(c)

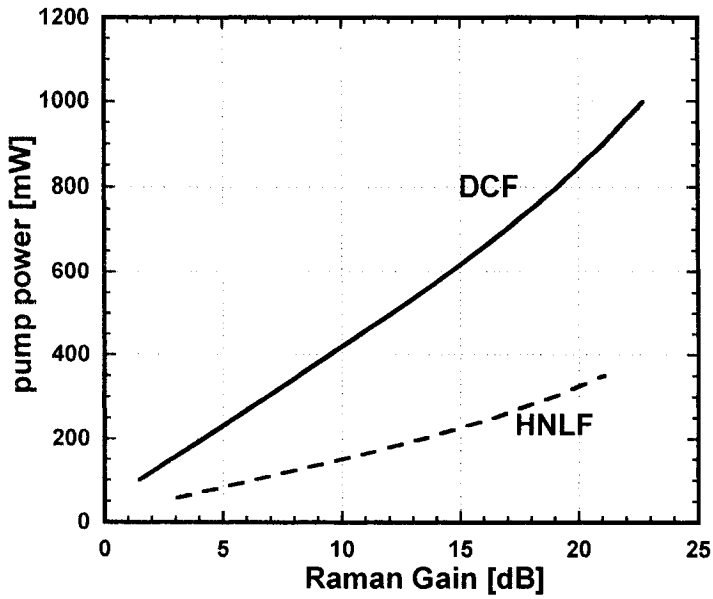
1200
1000
800
600
400
200
0
pump power [mW]
DCF
HNLF
0
5
10
15
20
25
Raman Gain [dB]

(d)

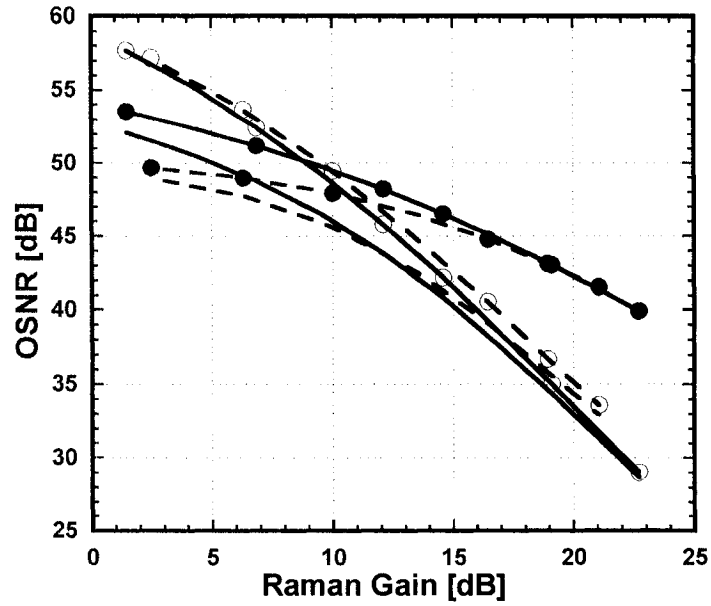

(e)

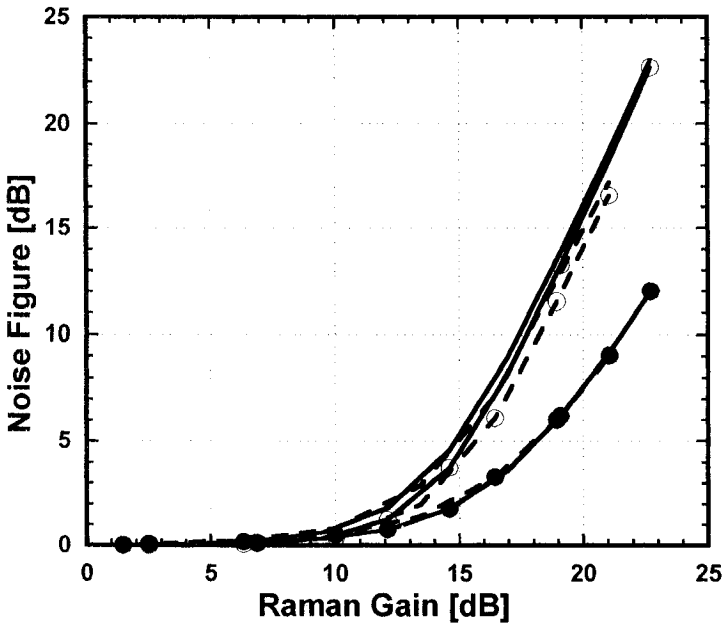

(f)

Figure 5.1 LRAs with 3000m DCF and HNLF as a gain medium

(a) gain vs. pump power; (b) OSNR vs. pump power; (c) noise figure vs. pump power; (d) pump power vs. gain; (e) OSNR vs. gain; (f) noise figure vs. gain

Dashed: HNLF; solid: DCF.

Blank circle: MPI noise only; black circle: ASE noise only.

From Figure 5.1, it can be seen that to reach a Raman gain of 20dB, the LRA with 3000m DCF requires 845mW pump power, while the LRA with 3000m HNLF needs only 324mW pump power, that's a saving of 62% on pump power. Generally, we can save 62% to 64% on pump power within the Raman gain range of 5 to 20 dB. This is a result directly from the high Raman gain efficiency of HNLF. The advantage in Raman gain coefficiency g_R / A_{eff}, 7.2 vs. 2.46 (1/W/km), leads to savings on pump power.

As for OSNR performance, those two LRAs achieve almost the same results. At the Raman gain of 20 dB, the LRA with HNLF has 1.4 dB advantages against the LRA with DCF. After separating the OSNR caused by ASE and MPI, we can see that in the large gain area(bigger than 10 dB), those two LRAs achieve same performance on OSNR induced by ASE only, and the OSNR performance advantage is caused by the signal induced MPI. With fixed length of gain fiber, OSNR performance is mainly decided by Raman gain. But in the small gain area, LRAs with DCF has some advantages on ASE noise performance, this might due to that gain power is distributed more equally along the fiber in LRAs with DCF.

We also get the similar results for noise figure. Comparing to OSNR, the difference on the noise figure performance is even smaller. This can be explained in a simple way: because we use same fiber length and same Rayleigh scattering coefficient for the Raman gain fibers, amplifiers have the same noise performance with the same Raman gain.

Here's some representative data for this simulation case: to reach a 15 dB Raman gain, a LRA with HNLF requires 220 mW pump power. At the same time, the LRA has 41 dB OSNR and 5dB noise figure. A LRA with DCF requires 620 mW pump power, achieves 40 dB OSNR and 5.1 dB noise figure.

5.2.2 Comparisons between LRAs with 900m or 3000m HNLF as a gain medium

In the first case, we see that a LRA with 3000m HNLF needs 324mW pump power to achieve a 20 dB Raman gain. To some extent, Raman gain increases with the increase of

the Raman gain fiber length as well as the pump power. We can compromise between fiber length and pump power while keeping the same Raman gain.

Our second case is to study the impact of the fiber length on LRA's Raman gain performance and noise characteristic. To be able to achieve 20 dB Raman gain with 1000mW pump power, the fiber length of HNLF for comparison is chosen to be 900m. We will compare LRAs with 900m or 3000m HNLF in this case and hope to see the relationships between fiber lengths, pump power and amplifier performance.

The simulation results are shown in Figure 5.2.

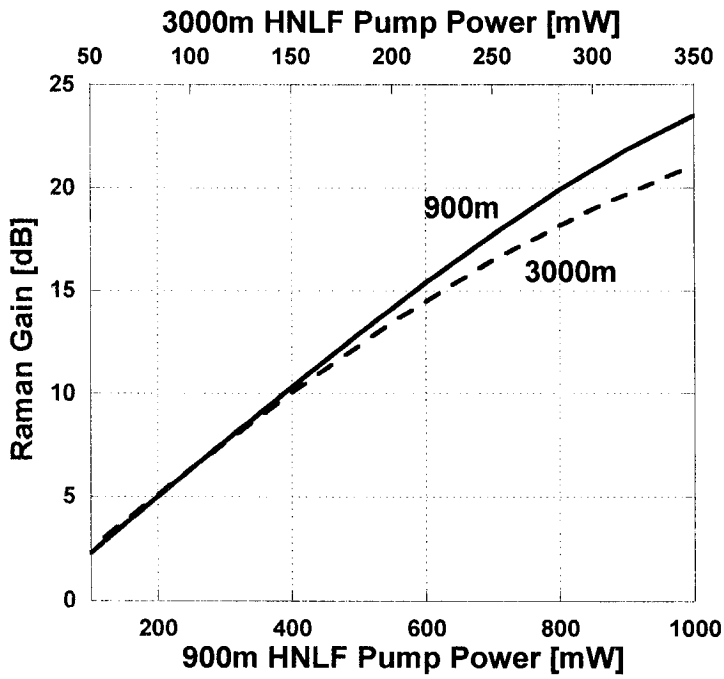

(a)

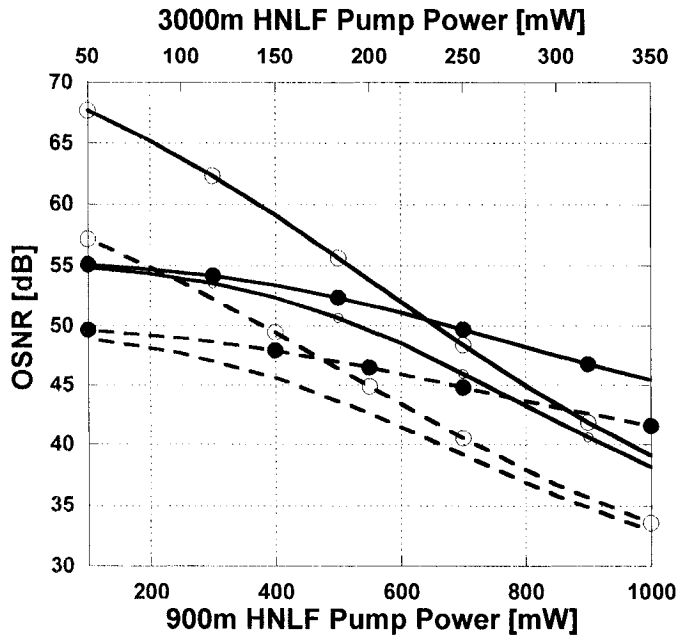
3000m HNLF Pump Power [mW]
50
100
150
200
250
300
350
70
65
60
55
50
45
40
35
30
OSNR [dB]
200
400
600
800
1000
900m HNLF Pump Power [mW]

(b)

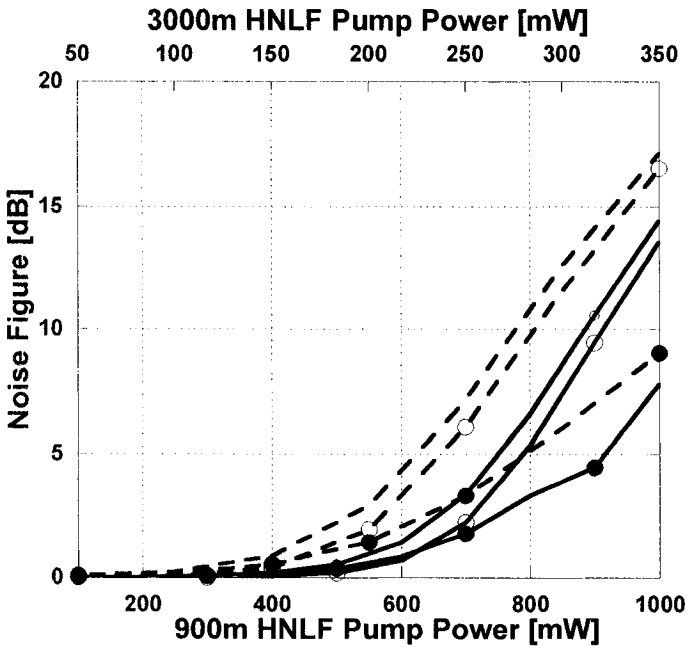
3000m HNLF Pump Power [mW]
50
100
150
200
250
300
350
20
15
10
5
0
Noise Figure [dB]
200
400
600
800
1000
900m HNLF Pump Power [mW]

(c)

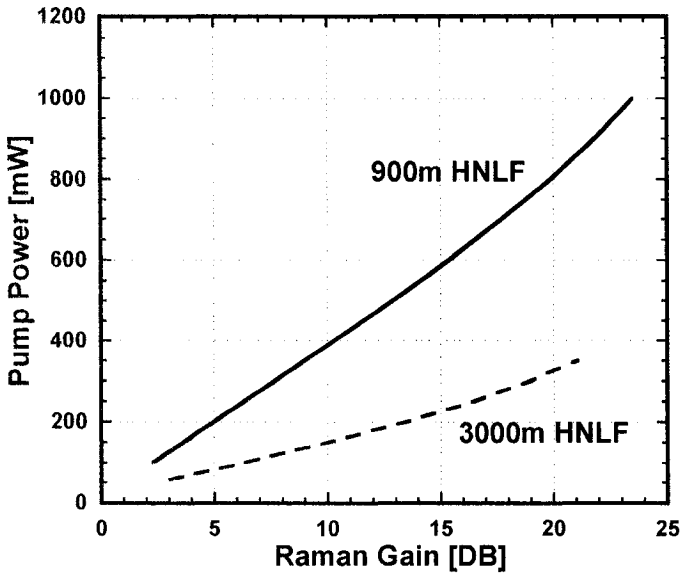
1200
1000
800
600
400
200
0
Pump Power [mW]
900m HNLF
3000m HNLF
0
5
10
15
20
25
Raman Gain [DB]

(d)

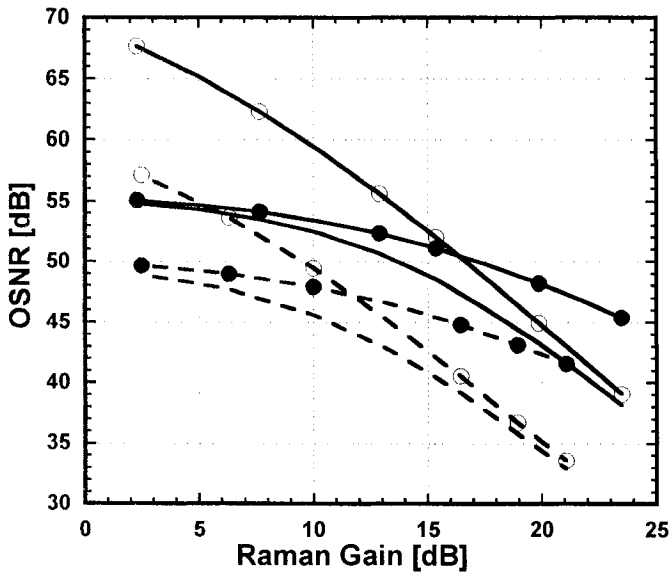
70
65
60
55
50
45
40
35
30
OSNR [dB]
0
5
10
15
20
25
Raman Gain [dB]

(e)

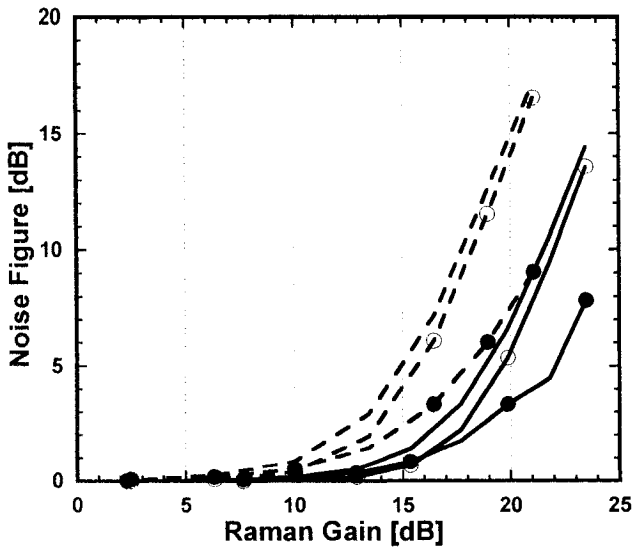

(f)

Figure 5.2 LRAs with 900m or 3000m HNLF as a gain medium

(a) gain vs. pump power; (b) OSNR vs. pump power; (c) noise figure vs. pump power; (d) pump power vs. gain; (e) OSNR vs. gain; (f) noise figure vs. gain

Dashed: 3000m HNLF; solid: 900m HNLF.

Blank circle: MPI noise only; black circle: ASE noise only.

From the figure above, we see that the LRA with 3000m HNLF needs 324.4 mW pump power to achieve a Raman gain of 20 dB, while the LRA with 900m HNLF requires 806mW pump power. 900m HNLF wastes part of pump power and 3000m HNLF uses pump power more efficiently. By using 3000m instead of 900m HNLF we can save 60% pump power; the expense is 3.3 times in Raman gain fiber length.

The drawback of using long Raman gain fiber is the downgrading on amplifiers' noise performance. For instance, with an amplifier Raman gain of 20 dB, the LRA with 900m HNLF obtains 43.1 dB OSNR and 6.84 dB noise figure value, the LRA with 3000m HNLF obtains 34.4 dB and 14.81 dB respectfully. Within the whole interested Raman gain range, a LRA with 900m HNLF achieves over 5 dB advantages on OSNR performance against a LRA with 3000m HNLF. We save on pump power and on the other

hand lose on amplifiers' noise performance. Noise performance is a very important character of optical amplifier. We need to choose the right Raman gain fiber length to get a balance between the pump power and the amplifier's noise characteristic.

As expected, signal induced MPI dominates an amplifier's noise performance in the large Raman gain area. For a LRA with 3000m HNLF, the turn point that MPI noise overcome ASE noise is 12 dB and for a LRA with 900m HNLF, the point is 16.8 dB. More discussions will be given in Section 5.3.

Here are some characteristic data for this simulation case: to achieve 15 dB Raman gain, a LRA with 900m HNLF needs around 590 mW pump power, and the LRA achieves 48.5 dB OSNR. The LRA's noise figure achieves 5 dB with a Raman gain of 18.8 dB.

5.2.3 Comparisons between LRAs with 3000m or 8000m DCF as a gain medium

We compared LRAs with different lengths of HNLF fibers in Section 5.2.2. To study the difference between DCF and HNLF, here in this section we compare LRAs with different lengths of DCF. We use the same method to choose fiber length as in Section 5.2.2; the fiber lengths of DCF for comparisons are 3000m and 8000m. Figure 5.3 shows the simulation results.

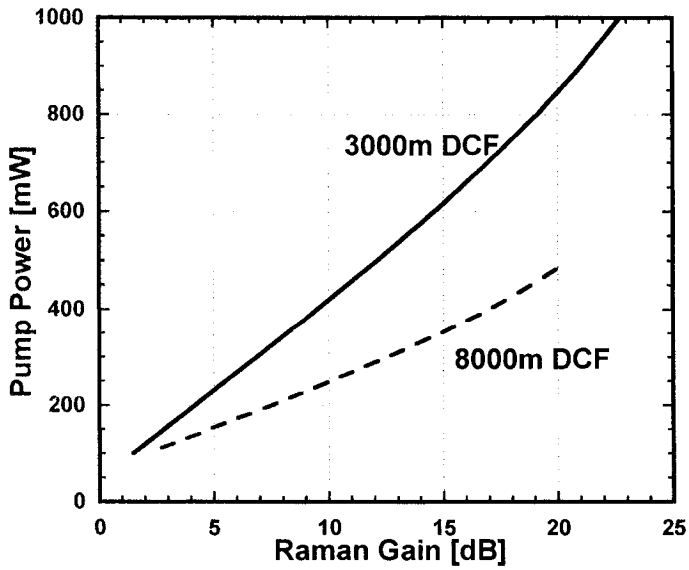

(a)

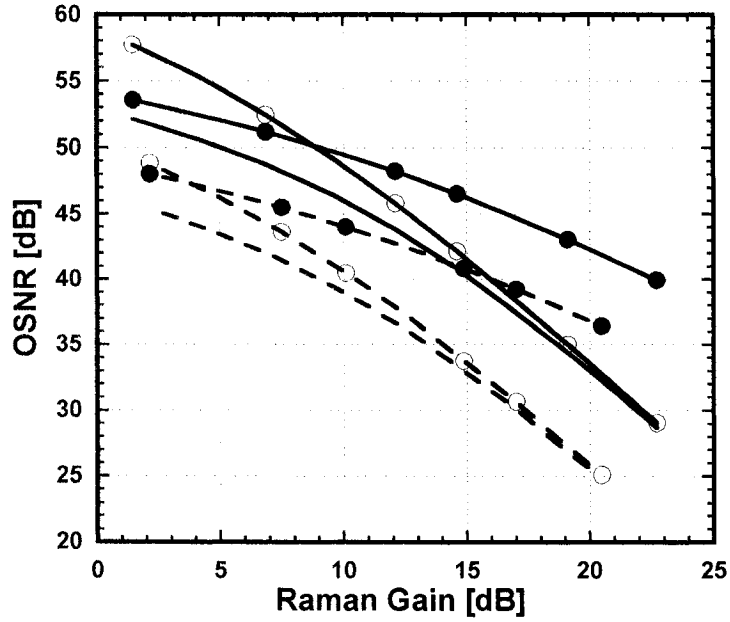

(b)

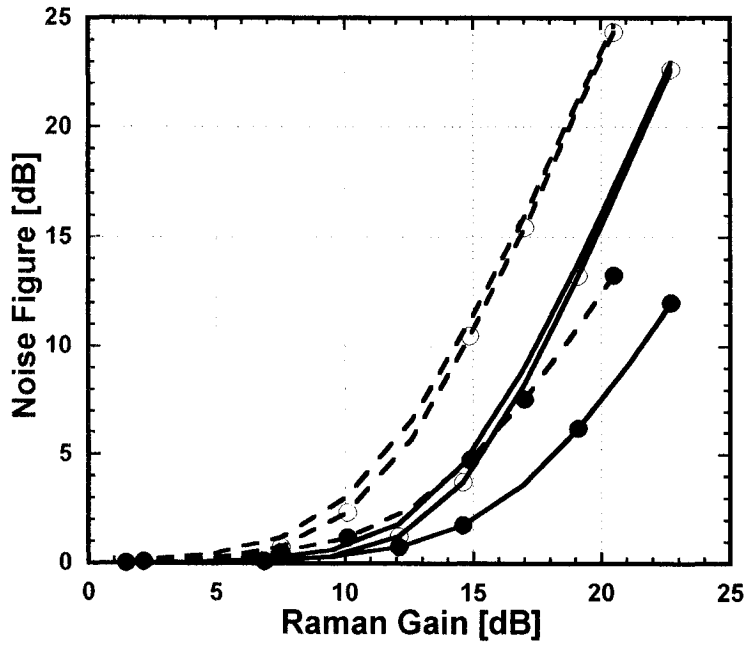

(c)

Figure 5.3 LRAs with 3000m or 8000m DCF as a gain medium

(a) Pump power (b) OSNR (c) noise figure

Dashed: 8000m DCF; solid: 3000m DCF.

Blank circle: MPI noise only; black circle: ASE noise only.

From Figure 5.3, we can see that a LRA with 8000m DCF save 43% (484.6 mW vs. 845.5 mW) pump power compared to a LRA with 3000m DCF to achieve a 20 dB gains, but loses 7.5 dB on the OSNR and 7.4 dB higher on the noise figure at the same time. That's a compromise between pump power savings and noise performance.

The results from simulations above and Section 5.2.2 shows that LRAs with DCF and LRAs with HNLF have similar character on relationships between fiber length, pump power and amplifier's noise performance. Longer fiber can utilize pump power more completely and leave less power wasted. We can save pump power by using long Raman gain fiber, and pump power can be efficiently used. The fallback is worse amplifier noise performance. We will give more discussions on the relationship between LRA's noise performance and Raman gain fiber length in Section 5.3.

5.2.4 Comparisons between LRAs with DCF or HNLF, fixed pump power 300mW

Till now, we used fixed length Raman gain fibers and changed pump power to study LRA's performance. In this case we will study the impact of Raman gain fiber length on the LRA's gain and noise performances; we will keep the pump power fixed and change the fiber length.

A 300mW single wavelength counter pump is chosen for the LRA, which can be considered as a low power Raman pump. The DCF fiber used for the LRA has a variable length between 3000m and 11000m, and HNLF fiber length varying from 900m to 3300m. With the fiber length range we chose, the two LRAs can achieve similar Raman gain performance because the comparisons have to be made with the same amplifier Raman gain. The simulation results are shown in the following figures.

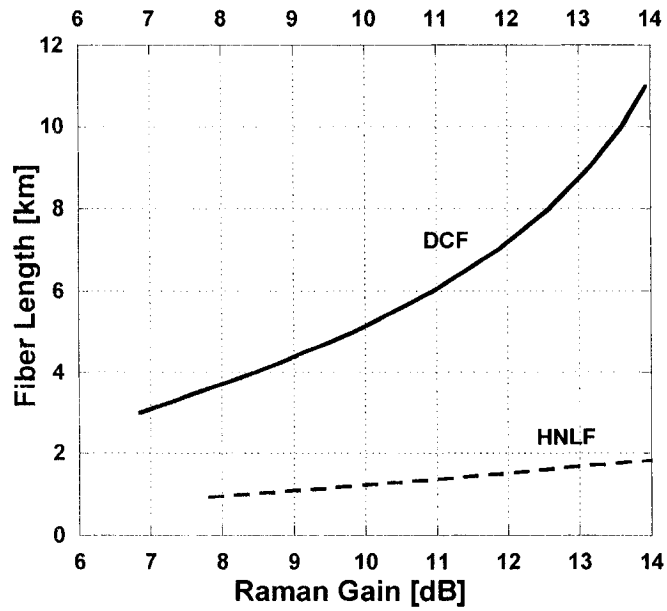
Fiber Length [km]
Raman Gain [dB]
DCF
HNLF
0
2
4
6
8
10
12
6
7
8
9
10
11
12
13
14

(a)

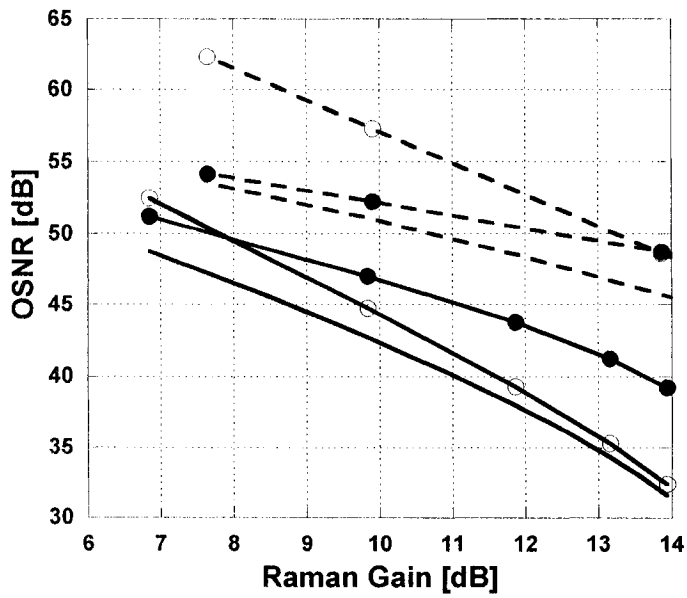
OSNR [dB]
Raman Gain [dB]
30
35
40
45
50
55
60
65
6
7
8
9
10
11
12
13
14

(b)

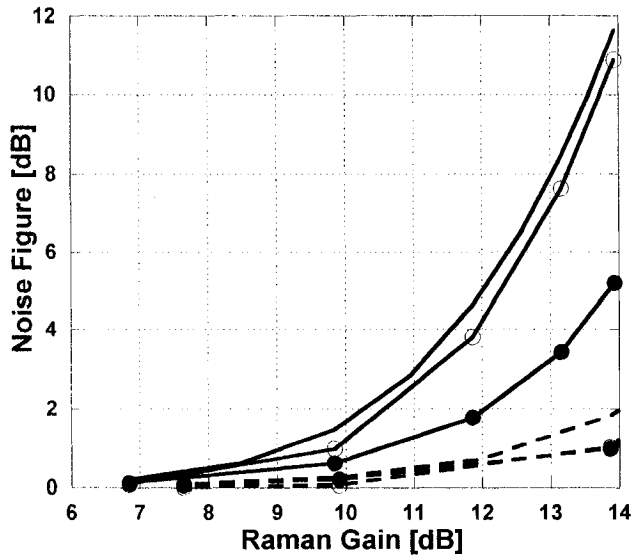

(c)

Figure 5.4 LRAs with DCF or HNLF, fixed 300mW pump power.

(a) Fiber length (b) OSNR (c) noise figure

Dashed: HNLF; solid: DCF.

Blank circle: MPI noise only; black circle: ASE noise only.

Figure 5.4 clearly shows the relationship between the fiber length and the amplifier's Raman gain. With the increase of fiber length, the Raman gain increases for both LRAs with DCF or HNLF. For a LRA with DCF, when the fiber length change from 3000m to 11000m, the amplifier's Raman gain increases from 6.85 dB to 13.94 dB. For a LRA with HNLF, when fiber length changes from 900m to 1800m, the amplifier's Raman gain increase from 7.65 dB to 13.87 dB. With the large Raman gain coefficiency value, HNLF is more efficient to achieve Raman gain compared to the fiber length change. In other words, a LRA with HNLF's Raman gain increases more sharply with the increase of Raman gain fiber length. It's possible to reach a 19 dB Raman gain with 300 mW pump power using 3000m HNLF as a Raman gain medium.

Figure 5.4 also shows the difference on Raman gain efficiency between HNLF and DCF. To reach a Raman gain of 10 dB, a LRA with HNLF needs 1213m fiber and a LRA

with DCF needs 5.14 km fiber. A LRA with DCF requires 4.24 times length of fiber compared to a LRA with HNLF. HNLF has higher Raman gain efficiency and needs shorter length of the Raman gain fiber than DCF. In this case, a LRA with HNLF achieves better noise performance than a LRA with DCF. At the Raman gain of 10 dB, the noise characteristic results for a LRA with HNLF and a LRA with DCF are: 50.9 dB vs. 42.4 dB on OSNR and 0.27 dB vs. 1.67 dB on noise figure. Also among the whole gain area, a LRA with HNLF's noise performance beats that of a LRA with DCF. The improvement increases with the increase of amplifier Raman gain. There will be more discussions on this in Section 5.3.

5.2.5 Comparisons between LRAs with DCF or HNLF, fixed pump power 400mW

Similar to the case in Section 5.2.4, instead of the 300mW low power single pump, we use a 400mW power single pump in this section to study the amplifier's performance in large gain area. The setups of this simulation case are the same as those in Section 5.2.4, and the results are shown below.

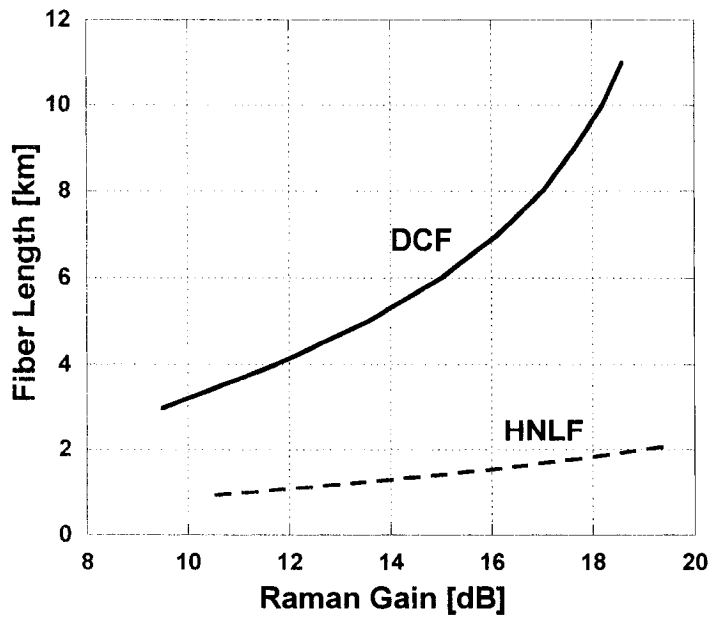

(a)

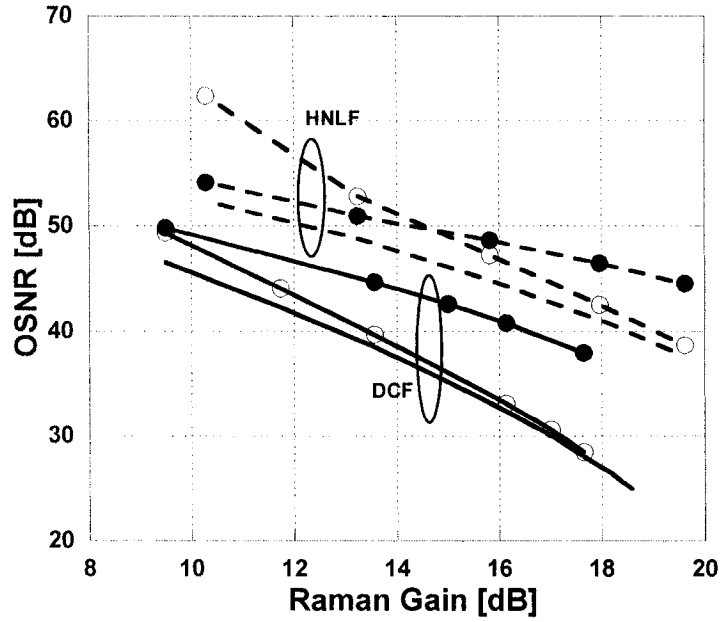

(b)

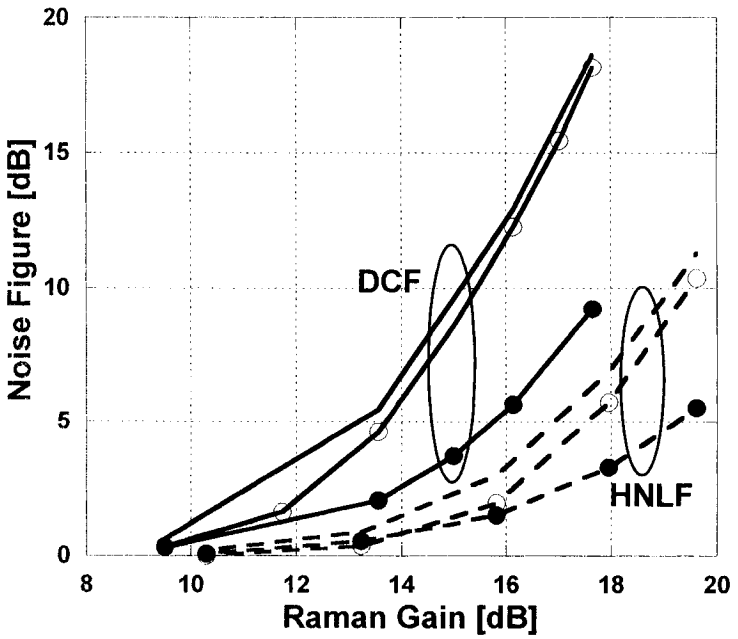

(c)

Figure 5.5 LRAs with DCF or HNLF, fixed 400mW pump power

(a) Fiber length (b) OSNR (c) noise figure

Dashed: HNLF; solid: DCF.

Blank circle: MPI noise only; black circle: ASE noise only.

We show the results in the following table for an amplifier Raman gain of 18 dB.

Table 5.3 LRAs with DCF or HNLF, fixed 400mW pump power

Item	LRA with HNLF	LRA with DCF
Fiber length required [m]	1805	9618
OSNR [dB]	40.96	27.04
Noise figure [dB]	6.95	28.65

The conclusions from Section 5.2.4 also apply here. HNLF has high Raman gain efficiency and a LRA with HNLF requires shorter length of Raman gain fiber than that of a LRA with DCF. With the same pump power and the same amplifier Raman gain, a LRA with HNLF achieves better noise characteristic than a LRA with DCF. Especially in large Raman gain area, where LRA's noise performance degrades quickly with the increase of Raman gain, a LRA with HNLF has an outstanding noise performance compared to a LRA with DCF. HNLF is a better substitute of DCF for LRA to remain acceptable noise performance when LRA reaches a large Raman gain.

5.2.6 Comparisons between LRAs with DCF or HNLF, fixed amplifier gain 15 dB

In this case, we study the relation between fiber lengths and pump power when LRAs have a fixed amplifier Raman gain of 15 dB. We change the Raman gain fiber length and the amplifier pump power at the same time to keep the same Raman gain. The simulation results are shown in the following figure.

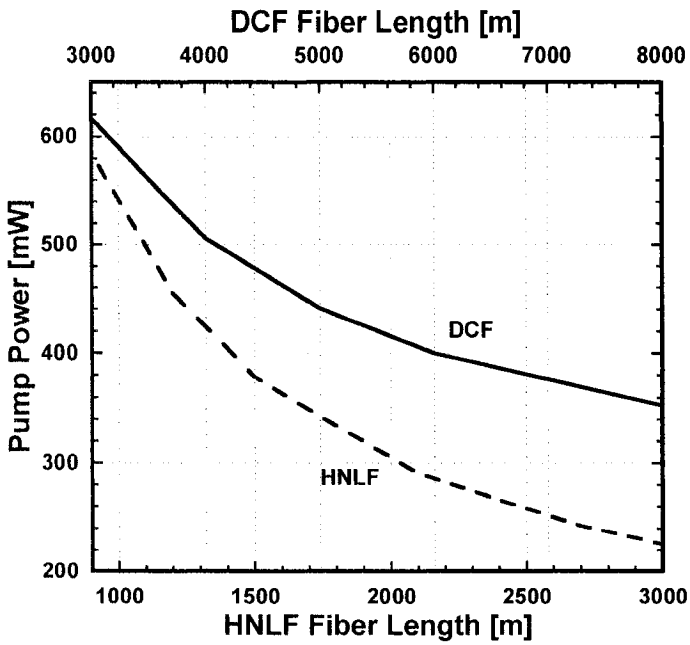
DCF Fiber Length [m]
3000
4000
5000
6000
7000
8000
600
500
400
300
200
Pump Power [mW]
DCF
HNLF
1000
1500
2000
2500
3000
HNLF Fiber Length [m]

(a)

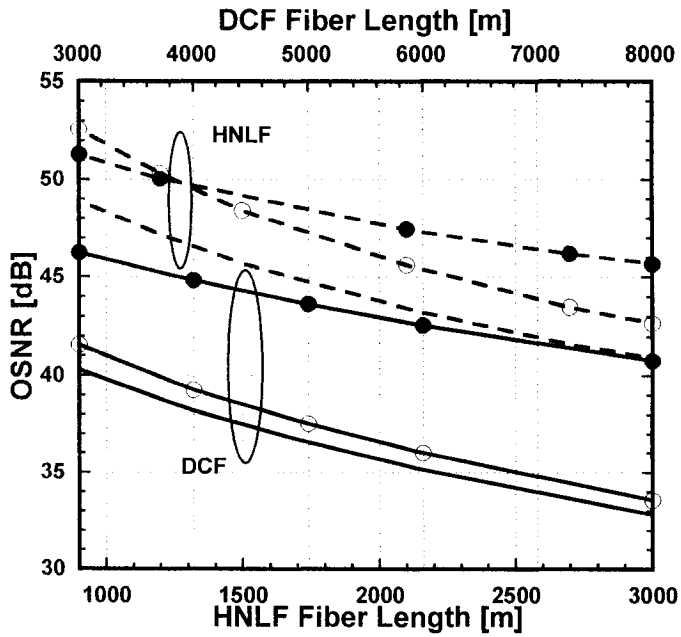
DCF Fiber Length [m]
3000
4000
5000
6000
7000
8000
55
50
45
40
35
30
OSNR [dB]
HNLF
DCF
1000
1500
2000
2500
3000
HNLF Fiber Length [m]

(b)

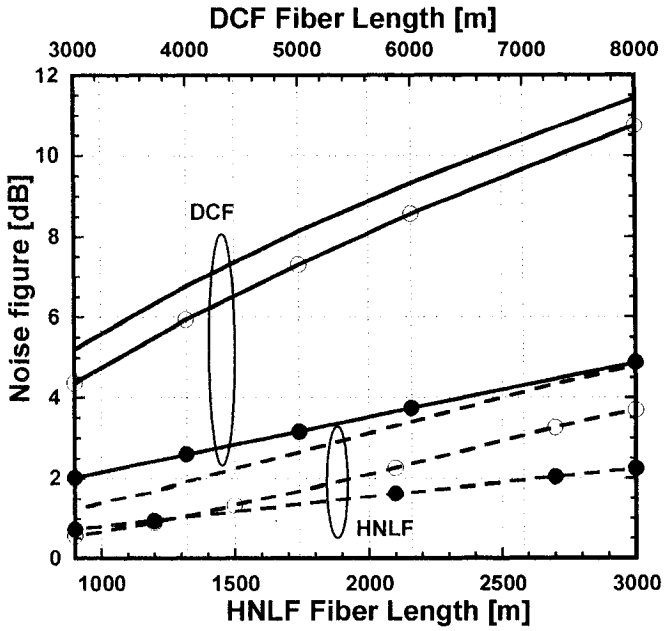

(c)

Figure 5.6 LRAs with DCF or HNLF, fixed 15 dB gain

(a) Pump power (b) OSNR (c) noise figure

Dashed: HNLF; solid: DCF.

Blank circle: MPI noise only; black circle: ASE noise only.

From the figure above, first we can see that HNLF has a higher Raman gain efficiency than DCF, as in other cases, a shorter length of fiber is required to achieve the same 15 dB Raman gain. Second, if we increase the fiber length, we need less pump power; this confirms the result from Section 5.2.2. But with more details, we can see the trend on how the fiber length and pump power affect each other in Figure 5.6.

Most importantly, Figure 5.6 clearly shows that when the amplifier Raman gain is 15 dB fixed, a LRA with HNLF always has better noise performance than a LRA with DCF in this case. A LRA with DCF requires longer Raman gain fiber than a LRA with HNLF. Its noise performance degrades quickly with the increase of gain. So a LRA with HNLF shows better results on noise characteristics than a LRA with DCF. Especially when a LRA works in the large Raman gain area, a LRA with HNLF can still remain acceptable

noise performance.

5.2.7 Comparisons between LRAs with DCF or HNLF, whole C band

All the above cases are focused on single 1552.18 nm channel; in this section the results for the whole C band are illustrated.

The settings are similar with other cases, and we use a 400mW power pump. To compare two LRAs with a similar Raman gain, we found 1415m HNLF has almost the same Raman gain efficiency with 6000m DCF. So a LRA with 1415m HNLF and a LRA with 6000m DCF are chosen to compare in this section. The following figure shows the result for 100 channels over C band, between 1530 and 1570 nm.

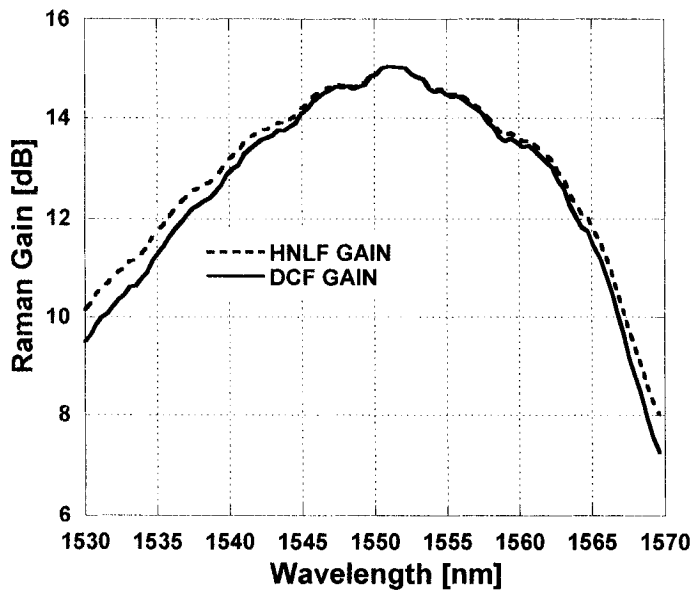

(a)

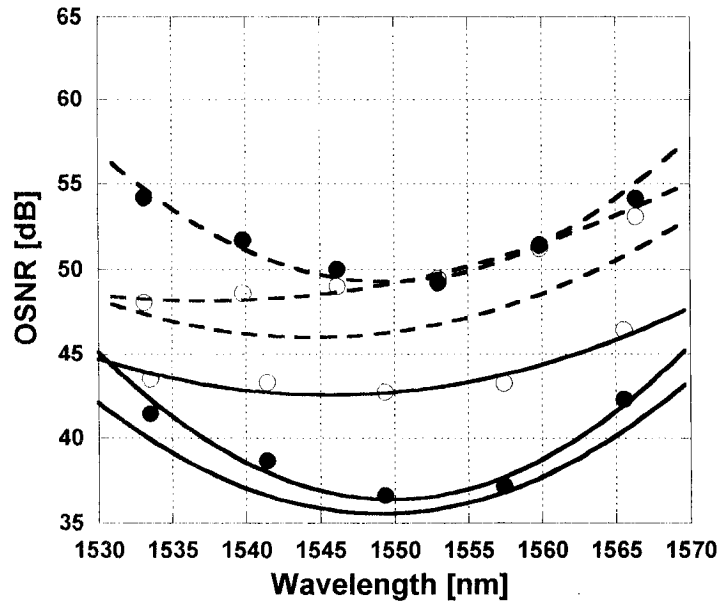

(b)

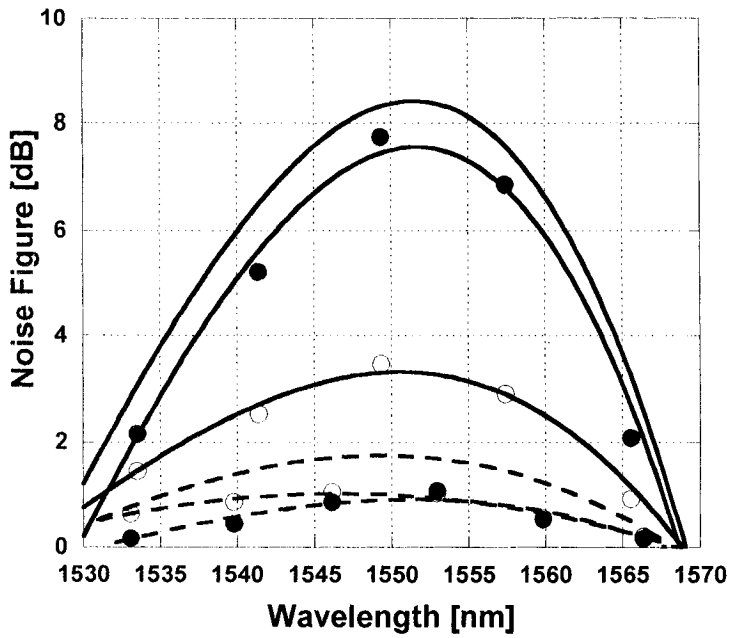

(c)

Figure 5.7 LRAs with DCF or HNLF, whole C band.

(a) Raman gain (b) OSNR (c) noise figure

Dashed: 1415m HNLF; solid: 6000m DCF.

Blank circle: MPI noise only; black circle: ASE noise only.

The following table shows the average value results over C band for those two amplifiers.

Table 5.4 LRAs with DCF or HNLF, whole C band

Amplifier performance	LRA with 1415m HNLF	LRA with 6000m DCF
Average gain [dB]	12.9	12.7
Average OSNR [dB]	47.7	40.0
Average noise figure [dB]	1.18	5.62
Gain ripple [dB]	7.02	7.76

A LRA with 1415m HNLF achieves similar gain performance over C band with a LRA with 6000m DCF, and shows better noise performance results. With about the same Raman gain, the LRA with 1415m HNLF achieves 7.7 dB advantages on average OSNR and 4.44 dB on average noise figure against the LRA with 6000m DCF.

The results are in match with results from other simulation cases for single C channel. Those conclusions apply to all channels over C band, not only the specified channel (1552.18 nm). From Figure 5.7 we can see the difference between the LRA with 1415 m HNLF and the LRA with 6000 m DCF reach maximum value on channel 1552.18 nm. When signal move to both ends of spectra, the Raman gain decreases, the difference also decreases.

5.2.8 Comparisons between different pumping schemes

We have studied different cases on LRAs with HNLF and LRAs with DCF, and all the cases are based on counter pump scheme. In real cases, we use not only counter pump, but also co-directional pump and bi-directional pump. In this section, we focus on whether the advantage of LRA with HNLF is independent of pump schemes.

Two LRAs are set up for simulations, one with 1415 m HNLF and the other one with 6000 m DCF. Instead of using counter pumping, we will simulate co-directional pumping

and bi-directional pumping. And for bi-directional pumping, pump power are equally divided between counter- and co- directional pumps.

The simulation results are as follows.

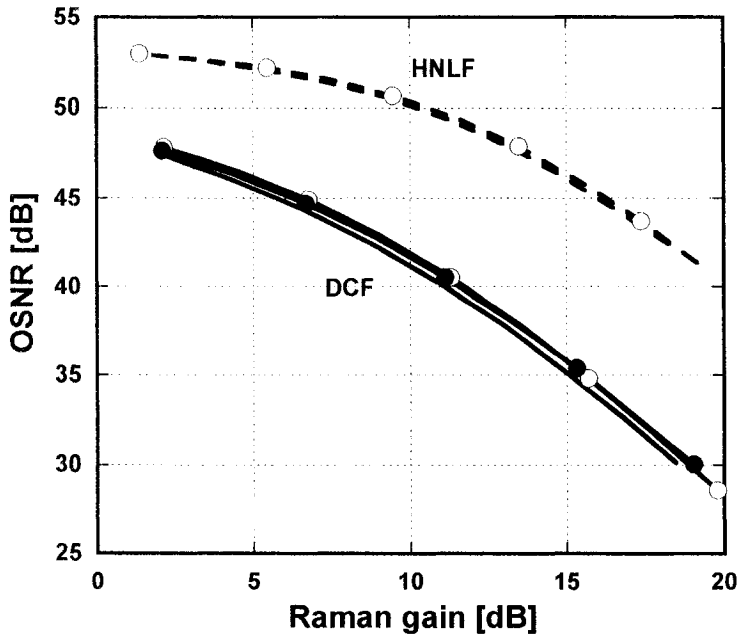

Figure 5.8 LRA with HNLF or DCF employing co- (blank circle), counter-, or bi-directional (black circle) pump.

The simulation results show that the noise performance in LRAs using HNLF or DCF is independent of pump schemes. There's very little difference between all 3 pumping methods for both LRA with HNLF and LRA with DCF. Since Fig. 3 only shows the OSNR for the channel at 1552.18nm, we expect that the pump schemes shall have impacts on the OSNR flatness over the C-band. However, the OSNR flatness optimization is beyond the intention of this study.

5.3 Conclusions and discussions

HNLF has a high Raman gain efficiency value up to 7.2 1/W/km; a LRA using HNLF as Raman gain medium can be implemented with short length fiber and packed into compact package.

A shorter length of HNLF can be used instead of DCF in LRA. Better amplifier noise performance i.e., higher OSNR and lower noise figure value, can be achieved with the same Raman gain. This is the most important conclusion in this thesis.

We can also use the same length of HNLF instead of DCF as a Raman gain medium, and save on the pump power. With a high Raman gain coefficiency, HNLF uses pump power more efficiently and a large portion of pump power can be saved. This is attractive in the cases where pump power or heat is a problem.

With better noise performance, a LRA with HNLF has smaller absolute value and thus a more flat noise characteristic. It would be easier in the design of transmission systems.

The advantage on noise performance of LRA with HNLF is independent of pumping schemes. No matter what pumping schemes we use, it's always possible to achieve better noise performance by replacing DCF with HNLF in LRA.

Now we talk about the theory explanations of LRA with HNLF as a Raman gain medium can achieve better noise performance. ASE and MPI noise theories and equations are given in chapter 3, which shows ASE and signal induced MPI noise accumulate along the fiber. High Raman gain efficiency of HNLF makes it possible to significantly reduce the length of LRA's Raman gain fiber. A shorter fiber length results in less chances beating of multiple delayed replicas of the signal or ASE, both signal and ASE induced MPIs are suppressed in LRA with HNLF compared to that in LRA with DCF. Therefore, noise performance of LRA with HNLF is improved considerably compared to LRA with conventional DCF. The advantages by using HNLF are especially clear in large amplifier Raman gain region where DRS dominates the whole amplifier's noise performance.

CHAPTER 6 Broad Band Amplification Using Multiple Pumps

In Chapter 5, we investigated LRAs with single wavelength pump. For broad band amplification, one pump wavelength is usually not enough; big gain ripple makes it impossible to achieve large Raman gain among the whole spectra. So in real cases, multiple pump wavelengths are implemented to get more flat gain and thus achieve broad band amplification. Multiple wavelength pumped fiber Raman amplifiers have recently been recognized as one of the key technologies to realize the ultra long haul broad band dense wavelength division multiplexing (DWDM) systems [20]. By appropriately choosing the pump spectrum, multiple wavelengths pumped FRA could provide a wide and flat gain band. In this chapter, we will investigate LRAs with 2 or 4 wavelengths pump.

6.1 Simulation cases and results for 2 pumps

In this section we use 2 counter pumps to amplify 184 channel (100 C band and 84 L band) signals over the spectra of 1530-1605 nm. Each input channel has a power of 0.01 mW (-20 dBm).

Two LRA models are set up, one LRA with 900m HNLF, and the other one with 3000m DCF. 2 pumps with a total power of 1200mW are implemented on each LRA. We optimized the pump wavelength and pump power to achieve the amplifier gain as flat as possible. The optimized pump wavelength and power are shown in the following table.

Table 6.1 Pump used for C+L band LRAs (2 pumps)

Pump wavelength	LRA with 900m HNLF	LRA with 3000m DCF
1442nm	822mW	850mW
1488nm	378mW	350mW

The simulation results are shown in Figure 6.1.

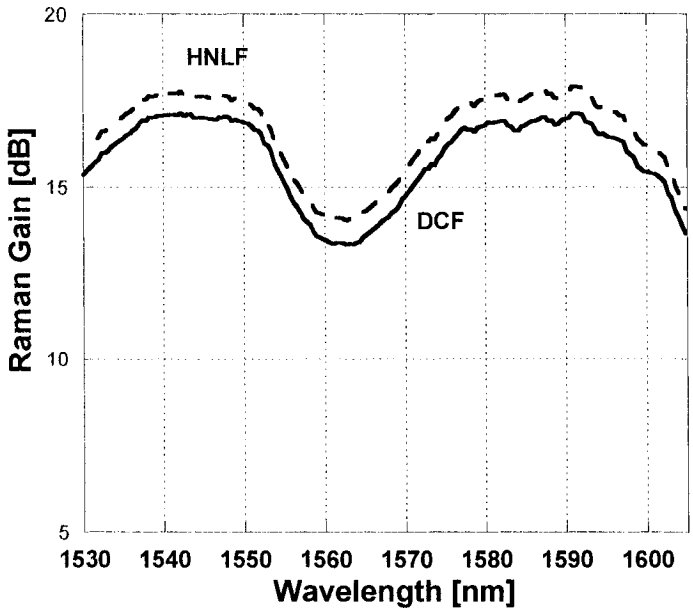
HNLF
DCF
Raman Gain [dB]
Wavelength [nm]
20
15
10
5
1530
1540
1550
1560
1570
1580
1590
1600

(a)

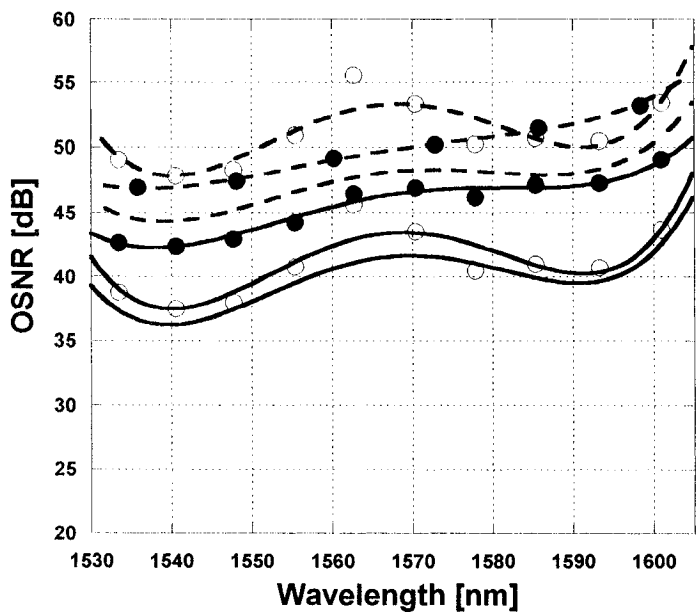
OSNR [dB]
Wavelength [nm]
60
55
50
45
40
35
30
25
20
1530
1540
1550
1560
1570
1580
1590
1600

(b)

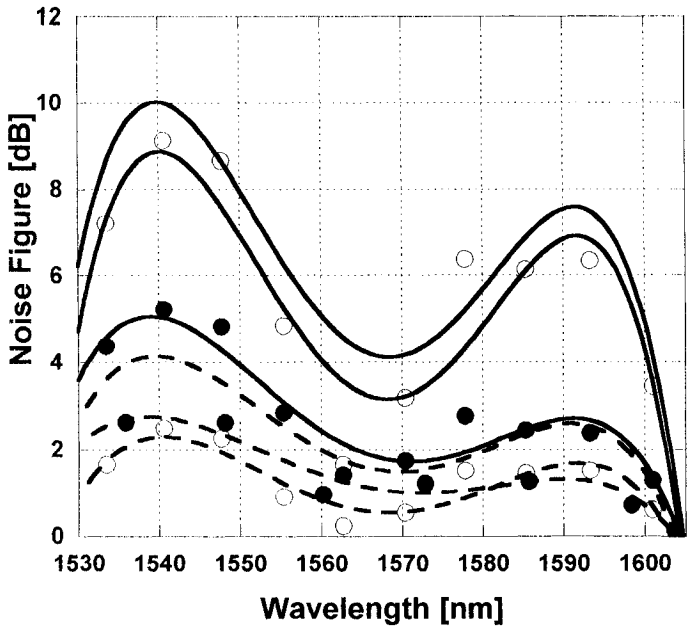

(c)

Figure 6.1 Comparisons between LRAs with 2 pumps

(a) Raman gain (b) OSNR (c) Noise figure

Dashed: LRA with 900m HNLF; solid: LRA with 3000m DCF:.

Blank circle: MPI noise only; black circle: ASE noise only.

Because of HNLF's high Raman gain efficiency, a LRA with 900m HNLF achieves same (or bigger) Raman gain than a LRA with 3000m DCF. And similar to cases in Chapter 5, a LRA with 900m HNLF performs better on amplifier's noise characteristics. The following table gives us the performance comparison results.

Table 6.2 Simulations results for 2 pumps

Performance	LRA with 900m HNLF	LRA with 3000m DCF
Average gain [dB]	17.1	15.9
Average OSNR [dB]	47.2	39.7
Average noise figure [dB]	2.45	6.51
Gain ripple [dB]	3.90	3.86

Like case 8 in Chapter 5, a LRA with 900m HNLF achieves better noise performance not only on one single channel, but also on the whole signal spectrum. High Raman gain efficiency makes a LRA with 900m HNLF capable of achieving big Raman gain, and short length fiber results in better noise performance compared to a LRA with 3000m DCF. With the same pump power, a LRA with 900m HNLF have 1.2 dB on average gain, 7.9 dB on average OSNR and 4.06 dB on average noise figure advantages against a LRA with 3000m DCF. This matches to our conclusions in Chapter 5.

6.2 Simulation cases and results for 4 pumps

6.2.1 LRAs with 900m HNLF or 3000mDCF

Using two pumps, we still have a large gain ripple (around 3.9 dB) in section 6.1. To get more flat gain, 4 pumps will be used in this section. All settings are the same as that in section 6.1.1, except that a 1200mW pump power will be divided into 4 pump wavelengths. The following table shows the optimized pump power and wavelength.

Table 6.3 Pump used for C+L band LRAs (4 pumps)

Wavelength [nm]	LRA using 1415 m HNLF [mW]	LRA using 3000 m DCF [mW]
1430	550	590
1447	190	185
1463	240	230
1496	220	195

The simulation results are shown in Figure 6.2.

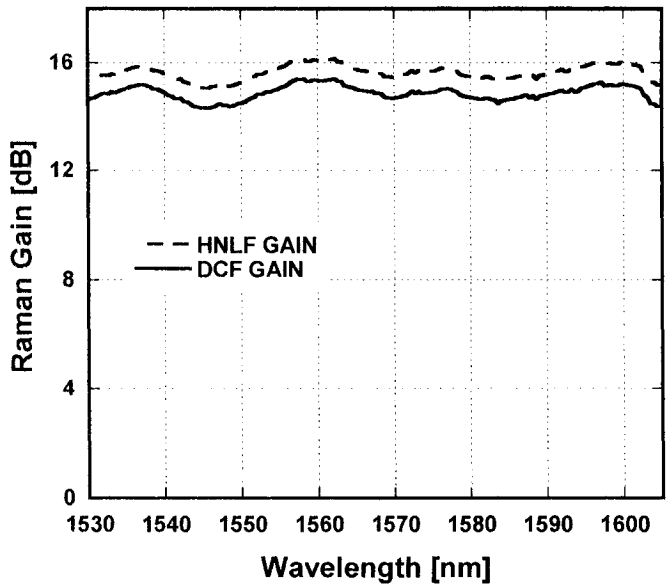
Raman Gain [dB]
16
12
8
4
0
HNLF GAIN
DCF GAIN
1530
1540
1550
1560
1570
1580
1590
1600
Wavelength [nm]

(a)

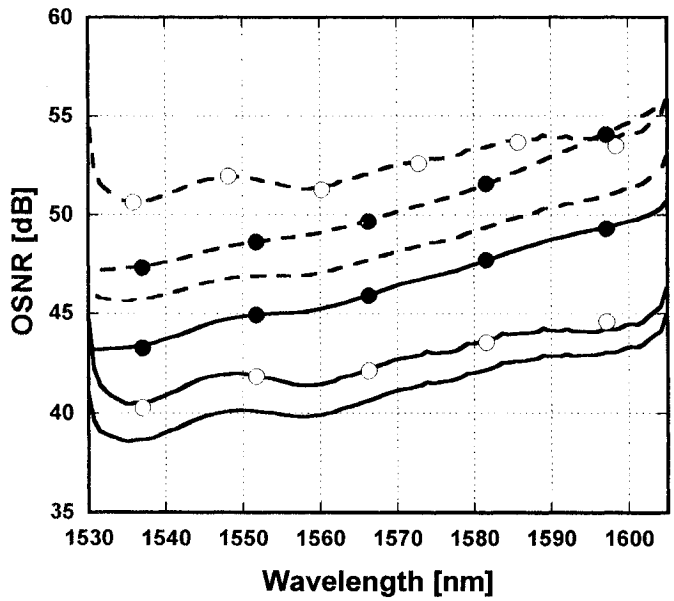
OSNR [dB]
60
55
50
45
40
35
1530
1540
1550
1560
1570
1580
1590
1600
Wavelength [nm]

(b)

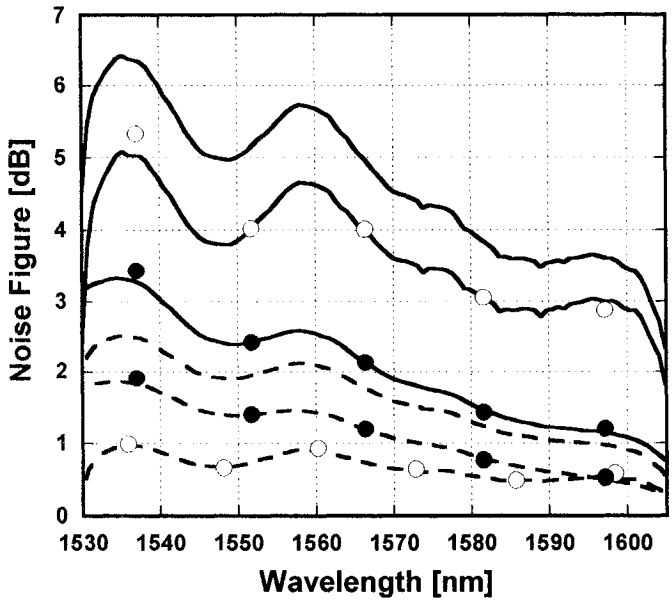

(c)

Figure 6.2 Comparisons between LRAs with 4 pumps

(a) Raman gain (b) OSNR (c) Noise figure

Dashed: 900m HNLF; solid: 3000m DCF.

Blank circle: MPI noise only; black circle: ASE noise only.

Comparing to the results from Section 6.1.1, we get much flatter Raman gain as well as OSNR and noise figure from LRAs with 4 pumps. We show results in the following table.

Table 6.4 Simulations results for 4 pumps

Performance	LRA with 900m HNLF	LRA with 3000m DCF
Average gain [dB]	15.6	14.9
Average OSNR [dB]	48.2	41.0
Average Noise figure [dB]	1.66	4.72
Gain ripple [dB]	1.08	1.10

The gain ripple decreased to around 1.1 db for LRAs with 4 pumps. Although the

average gain is a little bit smaller than that of LRA with 2 pumps, with a small gain ripple, this is more attractive to modern fiber communication systems. Again comparing these two LRAs with the same pump power, the LRA with 900m HNLF has bigger gain among C+L band than the LRA with 3000m DCF (15.6 dB vs. 14.9 dB on average gain). At the same time also achieves 7.2 dB advantages on average OSNR and 3.06 dB advantages on average noise figure. In one word, the LRA with HNLF achieves better noise performance with the same Raman gain than the LRA with DCF. This matches to our conclusions in chapter 5.

The LRA with HNLF also has flatter OSNR performance among C+L band than the LRA with DCF. With a smaller absolute value, there's smaller ripple on the OSNR value and it will be easier to compensate in transmission systems.

6.2.2 LRAs with 1415m HNLF or 6000mDCF

In Section 6.2.1, we use two LRAs with 900m HNLF or 3000m DCF. In this section, we will use LRAs with longer Raman gain fibers, 1415m HNLF or 6000m DCF. 1415m HNLF and 6000 m DCF have been proved to have similar Raman gain efficiency in Chapter 5. All settings remain the same as that in Section 6.2.1, except 1200mW pump power changes to 800mW as a result of the longer gain fiber. The following table is the optimized pump power and wavelength.

Table 6.5 Pump used for the C+L band (4 pumps)

Wavelength [nm]	LRA using 1415 m HNLF [mW]	LRA using 6000 m DCF [mW]
1430	375	420
1447	122	135
1463	170	133
1496	133	112

The simulation results are shown in Figure 6.3.

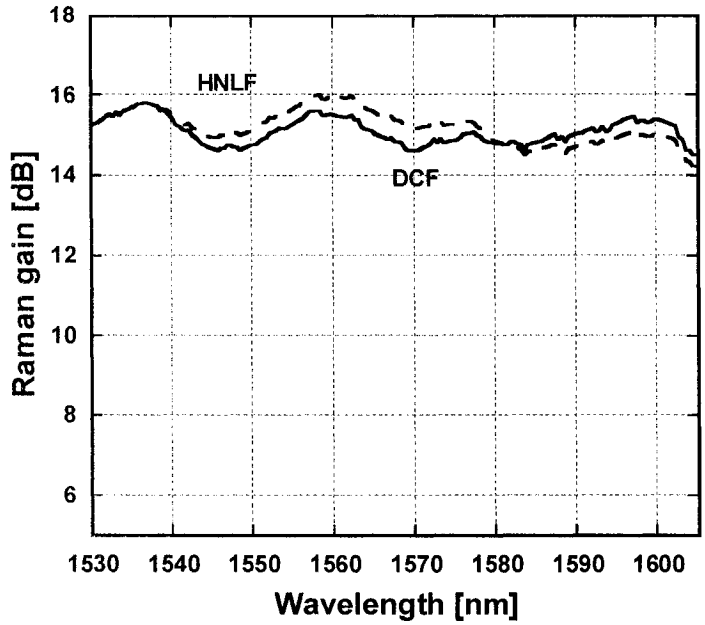
18
16
14
12
10
8
6
HNLF
DCF
Raman gain [dB]
1530
1540
1550
1560
1570
1580
1590
1600
Wavelength [nm]

(a)

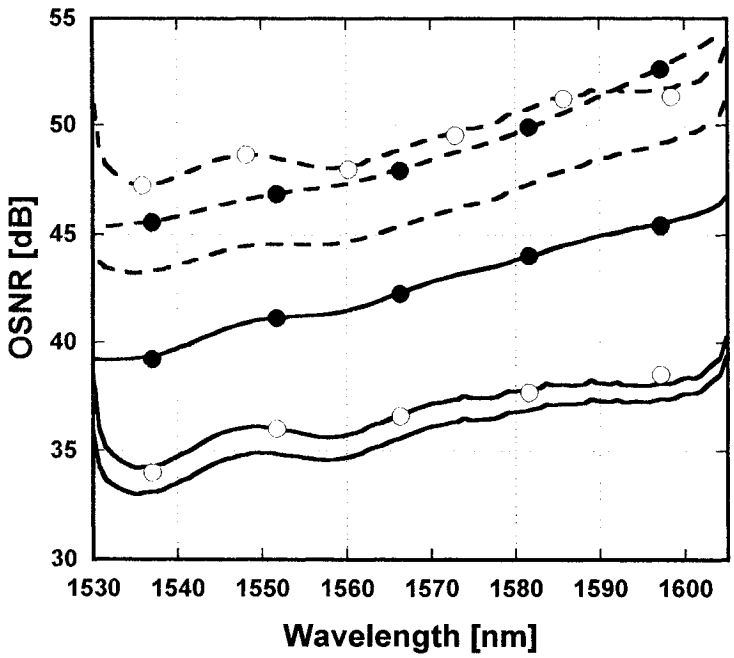
55
50
45
40
35
30
OSNR [dB]
1530
1540
1550
1560
1570
1580
1590
1600
Wavelength [nm]

(b)

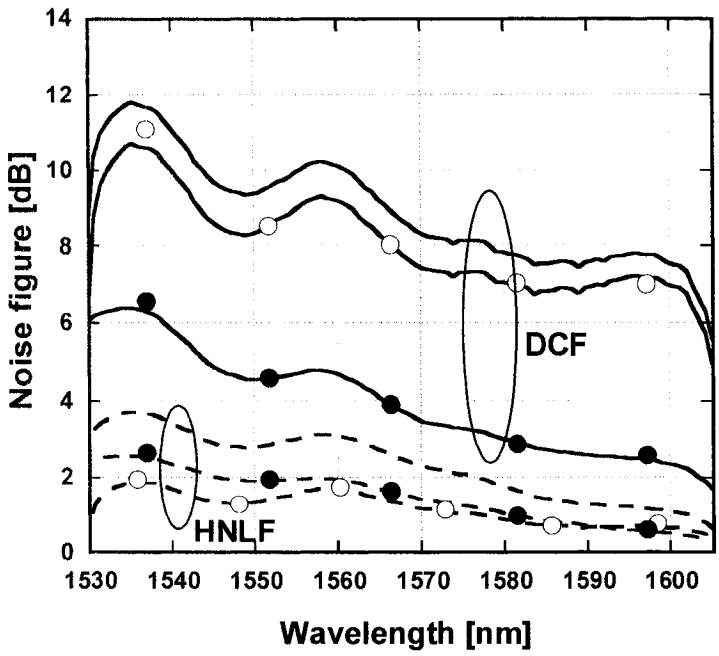

(c)

Figure 6.3 comparisons between LRAs with 4 pumps (longer fiber)

(a) Raman gain (b) OSNR (c) Noise figure

Dashed: 1415m HNLF; solid: 6000m DCF.

Blank circle: MPI noise only; black circle: ASE noise only.

The figure above shows that a longer Raman gain fiber uses the pump power more efficiently or completely, the LRAs with 800mW pump power achieve similar amplifier Raman gain with the LRAs with 1200mW pump power in Section 6.2.1. We have the following performance results table.

Table 6.6 Simulations results for 4 pumps

Performance	LRA with 1415m HNLF	LRA with 6000m DCF
Average gain [dB]	15.23	15.1
Average OSNR [dB]	46.0	35.6
Average Noise figure [dB]	2.36	9.05
Gain ripple [dB]	1.79	1.31

With the same pump power, the LRA with 1415m HNLF has almost the same amplifier Raman gain among C+L band with the LRA with 6000m DCF. In other word, we can say 1415m HNLF has same Raman gain efficiency with 6000 m DCF. Two LRAs achieve 15.23 dB and 15.10 dB on the average gain respectively. Again, a shorter fiber length in the LRA with 1115m HNLF results better noise characteristics than the LRA with 6000 m DCF. This matches to our conclusions from former parts. The results in Table 6.6 shows that a LRA with 1415m HNLF achieves 9.4 dB advantage on average OSNR and 6.69 dB advantage on average noise figure against a LRA with 6000 m DCF.

6.3 Conclusions and discussions

By using multiple wavelengths pump, we can realize a much flatter amplifier Raman gain. With only 2 wavelengths pump, the amplifier's Raman gain ripple drops to 3.9 db; with 4 wavelengths pump, the amplifier's Raman gain ripple drops to 1.1 dB. LRAs using multiple wavelengths pump can use pump power more efficiently or completely and achieve more effective Raman gain over the whole spectrum. Multiple wavelengths pump is the first choice for broad band optical amplification. In our cases, the signal spectrum is from 1530 to 1605nm, which has a bandwidth of 75 nm.

Multiple wavelengths pump monishes the different Raman gain between signal channels, and the difference between the absolute Raman gain value and the average Raman gain value is decreased. This results in an equally distribution of pump power and Raman gain among signals. Amplifiers' noise characteristics are improved in two aspects: the worst channel performance is improved and the performance among whole spectrum is more flat.

4 wavelengths pump results in a better Raman gain and noise characteristics performance than 2 wavelengths pump. Generally speaking, more wavelengths pump brings better performance. But on the other hand, more wavelengths pump is more difficult to design and interactions between pumps can degrade the signal channels. For

example, Raman pump-pump interactions transfer power from short- to long- wavelength pumps, causing a tilt in the signal noise figure as long- wavelength pumps penetrate further into the span than short wavelengths [20].

Again, a LRA with HNLF shows a higher Raman gain efficiency than a LRA with DCF. A big Raman gain can be generated with short length of HNLF. We showed that 900m HNLF can replace 3000m DCF and 1415 m HNLF can take place of 6000 m DCF in our cases. By using multiple wavelengths pumps we achieve broad band amplification. Our conclusions from Chapter 5 also apply to broad band signal spectrum. HNLF's high Raman gain efficiency remains effective for broad band spectrum with dense signal channels.

At the same time, using short length HNLF results in better noise performance, i.e. high OSNR and low noise figure value. LRAs with short length HNLF achieve better noise chrematistics than LRAs with conventional DCF. Our simulation results in this chapter matches to the result in Chapter 5 on single wavelength pump LRA.

With better noise performance, LRAs with HNLF also have flatter noise characteristic. There's smaller ripple on OSNR value and it will be easier to compensate in transmission systems if necessary.

CHAPTER 7 Impact of Rayleigh Scattering Coefficient on Amplifier's Noise Performance

We found the HNLF's Rayleigh scattering coefficient value range by repeating experiments in Chapter 4. In Chapter 5 and 6, we used the same Rayleigh scattering coefficient values for HNLF and DCF in our simulation cases. Rayleigh scattering coefficient is dependent on fibers, HNLF fiber from different manufactures or even from the same manufacture might have different values. In this chapter, we will study the influence of Rayleigh scattering coefficient on amplifiers' noise performance. In Section 7.1, some basic ideas about Rayleigh scattering coefficient will be given. Section 7.2 will be the simulation cases. Results and discussions will be demonstrated in section 7.3.

7.1 Introduction to Rayleigh scattering coefficient

Rayleigh scattering is a fundamental loss mechanism arising from local microscopic fluctuations in density. Silica molecules move randomly in the molten state and freeze in place during fiber fabrication. Density fluctuations lead to random fluctuations of the relative index on a scale smaller than the optical wavelength λ. Light scattering in such a medium is known as Rayleigh scattering [21]. The scattering cross section varies as λ^{-4}. As a result, the intrinsic loss of silica fibers from Rayleigh scattering can be written as: $\alpha_R = C/\lambda^4$, where the constant C is in the range 0.7-0.9 (dB/km)um^4,depending on the constituents of the fiber core[6].

Rayleigh scattering occurs in all fibers. A small part of light is always backscattered because of this phenomenon. Normally, this Rayleigh backscattering is negligible. However, it can be amplified over long lengths in fiber and affect the system performance in two ways. First, a part of backward propagating noise appears in the forward direction, enhancing the overall noise. Second, double Rayleigh scattering of the signal creates a

crosstalk component in the forward direction. It is this Rayleigh crosstalk, amplified by the Raman gain, which becomes the major source of power penalty. The fraction of signal power propagating in the forward direction after double Rayleigh scattering is the Rayleigh crosstalk [2]. This fraction is given by: $f_{DRS} = r_s^2 \int_0^L dz_1 G^{-2}(z_1) \int_{z_1}^{L} G^2(z_2) dz_2$ [22], where $r_s \sim 10^{-7}$ m^{-1} is the Rayleigh scattering coefficient, G(z) is the Raman gain at a distance z in the backward-pumping configuration for an amplifier of length L.

7.2 Simulation cases and results

Standard single mode fiber has a Rayleigh scattering coefficient value of around 1.17e-7 1/m (-39.32 dB/km)@1550nm, and the DCF used in our simulations has a value of 3.62e-7 1/m (-34.42 dB/km)@1550nm. From Chapter 4, we know that HNLF has a Rayleigh scattering coefficient value between -35.85 dB/km and -34.69 dB/km @1550nm. Here, we start our simulations with a value of 1.98e-7 1/m (-37.03 dB/km)@1550nm for HNLF. This value has considered Rayleigh scattering coefficient impact on fiber attenuation.

We increase the Rayleigh scattering coefficients value step by step and investigate the impact of Rayleigh scattering coefficients on the LRA's noise performance. The simulation case setups are the same as that in Section 5.1; fiber length for LRA with HNLF is 1415m. Simulation results are shown in Figure 7.1. A LRA with 6000m DCF is also shown in Figure 7.1 for comparisons. The Rayleigh scattering coefficient value R shown in Figure 7.1 is representative value on 1550nm.

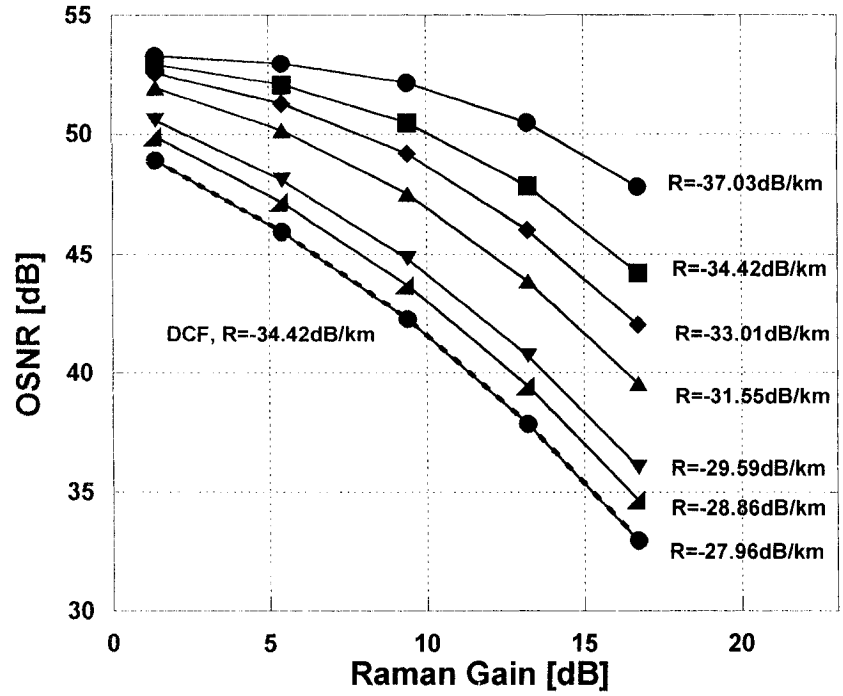

(a)

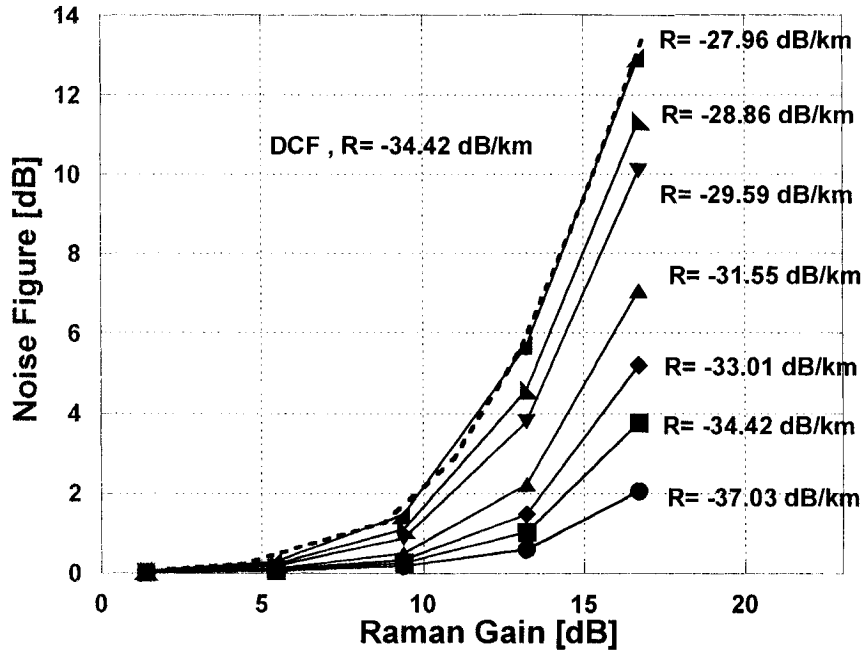

(b)

Figure 7.1 Impact of Rayleigh scattering coefficient on

(a) OSNR and (b) noise figure

Solid: 1415m HNLF dashed: 6000m DCF.

As expected, OSNR and noise figure performance degrade with the increase of Rayleigh scattering coefficient value. When the Rayleigh scattering coefficient is small, amplifier's noises remain in a low level even in big Raman gain area. We achieve 49 db OSNR and 1.4dB noise figure with a Raman gain of 15 dB, which is much better than the reference LRA with DCF. As the Rayleigh scattering coefficient increases to -27.96 dB/km@1550nm (~4.4 times of DCF which has a Rayleigh scattering coefficient of -34.4 dB/km), the noise performance advantage by using HNLF vanishes.

7.3 Conclusions and discussions

The Rayleigh scattering coefficient has a big impact not only on fiber's attenuation, but also on the LRA's noise performance. The noise performance advantage from LRA with HNLF against LRA with DCF comes from HNLF's high Raman gain efficiency, and it is independent of HNLF's Rayleigh scattering coefficient value. The high Raman gain character of HNLF makes it more flexible on Rayleigh scattering coefficient, even with a high Rayleigh scattering coefficient value, a LRA with HNLF can still remains the same noise level as a LRA with DCF.

With small Rayleigh scattering coefficient HNLF, it's possible to implement LRA with a high Raman gain with the noise characteristic controlled in an acceptable range. We showed that when HNLF has a Rayleigh scattering coefficient value of 1.98e-7 1/m (-37.03 dB/km)@1550nm, which is 1.6 times of standard single mode fiber, LRA can achieve 15 dB Raman gain with 49 dB OSNR. This may motivate us to invent HNLF with high Raman gain efficient, low fiber attenuation and low Rayleigh scattering coefficient.

CHAPTER 8 Conclusions

In this thesis, we theoretically investigate the amplifier Raman gain and noise characteristics performance for LRA utilizing highly nonlinear fiber with a high Raman gain coefficient (7.2 1/W/km) and low fiber attenuation (<0.6 dB/km from 1480 to 1680 nm). Comparisons with LRA using conventional DCF are given. The following conclusions can be drawn from our work.

1. Raman amplifier modeling

A set of Raman propagation equations is given, which describes the forward and backward power evolutions along the fiber for pumps, signals, and amplified spontaneous emission (ASE), including the effects due to Rayleigh backscattering, Stokes and anti-Stokes spontaneous emission. The 4^{th}-order Runge-Kutta method was used to solve the differential equations. The scaled Raman gain coefficients are used to accurately model the Raman gain coefficients for different pump wavelengths.

We verified our results against published experimental results, and our modeling on Raman fiber amplifier and DRS noise are proved to be accurate.

2. High Raman gain efficiency of HNLF

Highly non-linear fiber is a fiber with high non-linearity to generate Raman gain efficiently and used as a gain medium for the lumped Raman amplifier. Our work proved that HNLF can be used in lumped fiber Raman amplifiers. Compared to standard single mode fiber and dispersion compensating fiber, HNLF has much bigger Raman gain efficiency. A short length of HNLF (in the range of 1-2 km) can generate big Raman gain.

With high Raman gain efficiency, HNLF can use pump power more efficiently. With the same length of amplifier Raman gain fiber, less pump power is required for the LRA with HNLF than LRA with DCF to achieve the same Raman gain. With the same pump

power, a shorter length of Raman gain fiber is needed for the LRA using HNLF than LRA using DCF to achieve the same Raman gain.

A short length of Raman gain fiber makes it possible to pack a LRA into a compact package.

3. Improvements on ASE noise with LRA using HNLF

ASE noise accumulates along the fiber in LRA. Backward traveling ASE will be reflected in the forward direction and experience gain before reaching the receiver. This as well as spontaneous emission experiencing multiple reflections will degrade the signal-to-noise ratio [23].

There is less chance for the beating of signal and ASE noise with a short length of Raman gain fiber. Thus results a suppressed ASE noise in LRAs using HNLF as a gain medium. This mainly affects the LRA's noise performance in small Raman gain area.

4. Improvements on DRB noise with LRA using HNLF

Rayleigh scattering can occur in an optical fiber due to small inhomogeneities or microscopic variations in the refractive index. Portion of the signal is backscattered by Rayleigh scattering process and it suffers the gain, supplied by Raman pumping, more than twice before it is combined with the signal. Because of their long lengths and their nonuniform gain distribution, fiber Raman amplifiers (FRA) are more likely to suffer from generation of double Rayleigh backscattering(DRB). Noise due to DRS of the signal in the gain fiber is one of the most significant limiting factors in the design of a Raman amplifier.

When HNLF is implanted in LRA, high Raman gain coefficient makes it possible to use short length Raman gain fiber. With short length of Raman gain fiber, there's less chance for the beating of signal and its reflected replica. Thus results a suppressed DRB noise in LRAs with HNLF fiber. By using HNLF as a Raman gain medium, significantly

improvements on LRA's noise performance can be achieved.

5. Rayleigh scattering coefficient impact on amplifier noise performance

Rayleigh scattering coefficient has a big impact not only on fiber's attenuation, but also on LRA's noise performances. The high Raman gain character of HNLF makes it more flexible on the Rayleigh scattering coefficient. Even with a high Rayleigh scattering coefficient value (4.5 times of DCF), LRA with HNLF can remain the same noise level as LRAs with DCF.

The noise performance advantage from a LRA with HNLF against a LRA with DCF comes from the HNLF's high Raman gain efficiency, and it's independent of HNLF's Rayleigh scattering coefficient value.

Improvement on HNLF's Rayleigh scattering coefficient is one way to achieve lower noise LRA.

6. Future development of HNLF

From our works, we can see that the improved noise performance of LRA with HNLF is independent of Rayleigh scattering coefficient. Better noise performance can be achieved with the implement of HNLF with higher Raman gain efficiency. This points out a way for making a high gain and low noise Raman amplifier.

As we mentioned in chapter 4,

$$G_R\ [dB]=10\log[\exp(\frac{g_R}{A_{eff}}P_p\ L_{eff})$$

And we have:

$$\text{nonlinearity coefficient}\ \gamma \propto \frac{n_2}{A_{eff}} = \frac{\text{nonlinear index}}{\text{effective area}}$$

A fiber with small A_{eff}, high N_A, and low attenuation α is desirable for high G_R.

To achieve small effective area, we can use: [24]

- Tapered fibers

- Holey fibers (HF)
- Hole-assisted lightguide fibers (HALF)
- Photonic-crystal fiber (PCF)

As for highly-nonlinear materials, we can use: [24]

- Tellurite
- As2O3
- BiO2
- Etc.

With the new ideas and designs, it's possible to raise the Raman gain parameter g_R / A_{eff} to go beyond the best HNLF.

References

[1] G. Agrawal, "Fiber-Optic Communication Systems: Amplifier Performance," *Chapter 6, The Institute of Optics University of Rochester, Rochester, NY. Third edition, pp. 22, 2002.*

[2] M. N. Islam, "Raman Amplifiers for Telecommunications," *IEEE J. Selected Topics in Quantum Electron. vol.8, pp.548-559, 2002.*

[3] T. Miyamoto, M. Tanaka, J. Kobayashi, T. Tsuzaki, T. Okuno, M. Kakui and M. Shigematsu, "Development of Highly-nonlinear-fiber-based Raman Amplifier for CWDM Transmission Systems", *SEI Technical Review, No. 57, pp. 6-11, Jan. 2004.*

[4] R. Stolen and E. Ippen, "Raman Gain in Glass Optical Waveguides," *Appl. Phys. Lett., vol.22, pp. 276-278, 1973.*

[5] L. Mollenauer, J. Gordon, and M. Islam, "Soliton Propagation in Long Fibers with Periodically Compensated Loss," *IEEE J. Quantum Electron. vol.22, pp. 157-173, 1986.*

[6] J. Bromage, "Raman Amplification for Fiber Communications Systems," *IEEE J. Lightwave Technology, vol.22, pp. 79-93, Jan., 2004.*

[7] N. Gryspolakis, L. R. Chen and T. Zambelis, "Two-stage Discrete Fiber Raman Amplifiers with and without Gain-clamping", *22nd Queen's University Biennial Symposium on Communications, 1-3 June 2004, Kingston, Ontario, paper 149.*

[8] K. Nagayama, M. Matsui, M. Kakui, T. Saitoh, K. Kawasaki, H. Takamizawa, Y. Ooga, I. Tsuchiya and Y. Chigusa, "Ultra Low Loss (0.1484 dB/km) Pure Silica Core Fiber", *SEI Technical Review, No. 57, pp. 3-6, Jan. 2004.*

[9] J. Bouteiller, K. Brar, S. Radic, J. Bromage, Z. Wang, C. Headley, "Dual-order Raman Pump Providing Improved Noise Figure and Large Gain Bandwidth," *OFC 2002, PD FB3.*

[10] R. Stolen, "Optical Fiber Telecommunications," *Chapter 5, pp.127-133. Academic Press, New York, 1979.*

[11] P. Parolari, L. Marazzi, L. Bernardini, and M. Martinelli, "Double Rayleigh Scattering Noise in Lumped and Distributed Raman Amplifiers", *IEEE J. Lightwave Technology, Vol. 21, pp. 2224-2228, Oct. 2003.*

[12] C. Raman and K. Krishnan, "A New Type of Secondary Radiation", *Nature, vol.121, pp.501, 1928.*

[13] C. Zhao, Z. Li, X. Yang, C. Lu, W. Jin, and M. S. Demokan, "Effect of A Nonlinear Photonic Crystal Fiber on the Noise Characterization of A Distributed Raman Amplifier", *IEEE photonics Technology Letter, Vol. 17, pp. 561-563, Mar. 2005.*

[14] K. Rottwitt, A. Stentz, L. Leng, M. Lines, H. Smith, "Scaling of the Raman Gain Coefficient: Applications to Germanosilicate Fibers", *IEEE J. Lightwave Technology, vol.21, pp. 1652-1662, July 2003.*

[15] I. Mandelbaum, M. Bolshtyansky, "Raman Amplifier Model in Single-mode Optical Fiber," *IEEE Photonics Technology letter, vol.15, pp. 1704-1706 , Dec. 2003*

[16] P. B. Hanson, L. Eskildsen, A. J. Stentz, T. A. Strasser, J. Judkins, J. J. DeMarco, R.Pedrazzani, and D.J. DiGiovanni, "Rayleigh Scattering Limitations in Distributed Raman Pre-amplifiers", *IEEE Photonics Technology letter, vol. 10, pp159-161, Jan, 1998.*

[17] C. R. S. Fludger and R. J. Mears, "Electrical Measurements of Multipath Interference in Distributed Raman Amplifiers," *IEEE J. Lightwave Technology, vol. 19, pp. 536–545, Apr., 2001.*

[18] S. A. E. Lewis, S. V. Chernikov, and J. R. Taylor, "Characterization of Double Rayleigh Scatter Noise in Raman Amplifiers," *IEEE Photonics Technology letter, vol. 12, pp. 528–530, May, 2000.*

[19] "HNLF for discrete Raman gain," *SEI, http://www.sei.co.jp/fbr-opt-eng/specialty/hnlf/pdf/hnlf.pdf*

[20] S. Cui, J. Liu, and X. Ma, "A Novel Efficient Optimal Design Method for Gain-flattened Multiwavelength Pumped Fiber Raman Amplifier", *IEEE Photonics Technology letter, vol. 16, pp. 2451-2453, Nov., 2004.*

[21] M. Born and E. Wolf, "Principles of Optics", *7th edition, Cambridge University Press, New York, 1999.*

[22] M. Nissov, K. Rottwitt, H. D. Kidorf and M.X. Ma, *Electron Lett. 35, 997 (1999).*

[23] P. B. Hanson, L. Eskildsen, A. J. Stentz, T. A. Strasser, J. Judkins, J. J. DeMarco, R.Pedrazzani, and D.J. DiGiovanni, "Rayleigh Scattering Limitations in Distributed Raman Pre-amplifiers", *IEEE Photonics Technology letter, vol. 10, pp159-161, Jan, 1998.*

[24] L. G. kazovsky and M. E. Marhic, "Toward 100Tb/s Communication on a Single Optical Fiber', *http://oclab.usc.edu/nsf/oct2002/pdf/marhic-100tbps.pdf.*

Appendix A : Fiber Data Used in This Thesis

A.1: Raman gain coefficiency

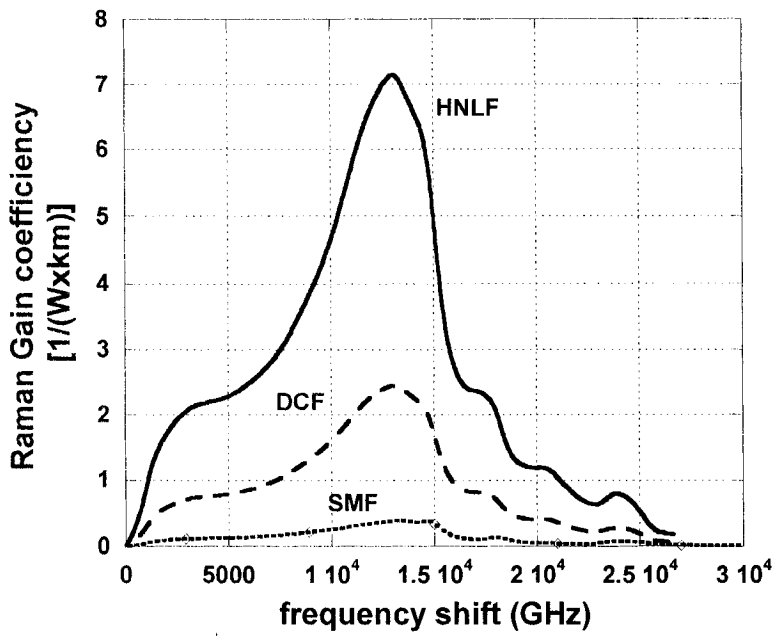

Figure a.1: Raman gain coefficiency of HNLF, DCF and SMF

A.2: Fiber loss

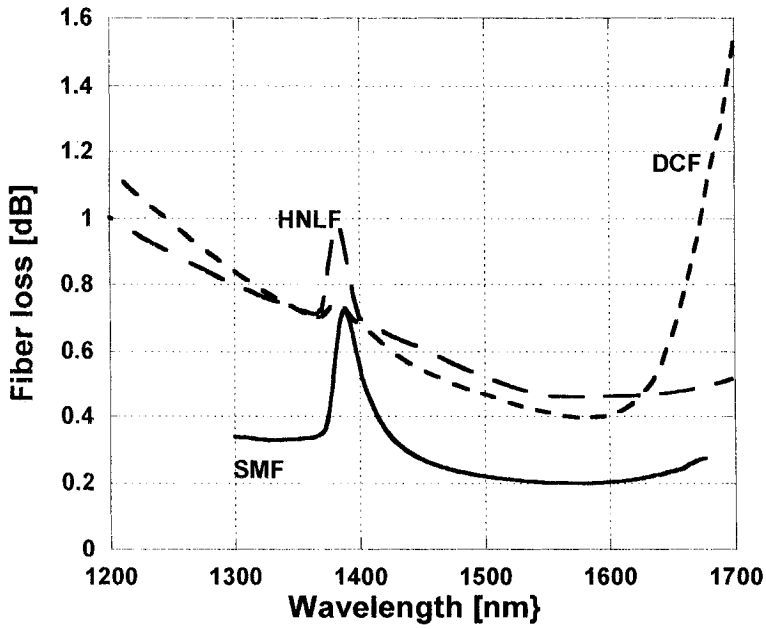

Figure a.2: fiber loss of HNLF, DCF and SMF

A.3: Rayleigh scattering coefficient

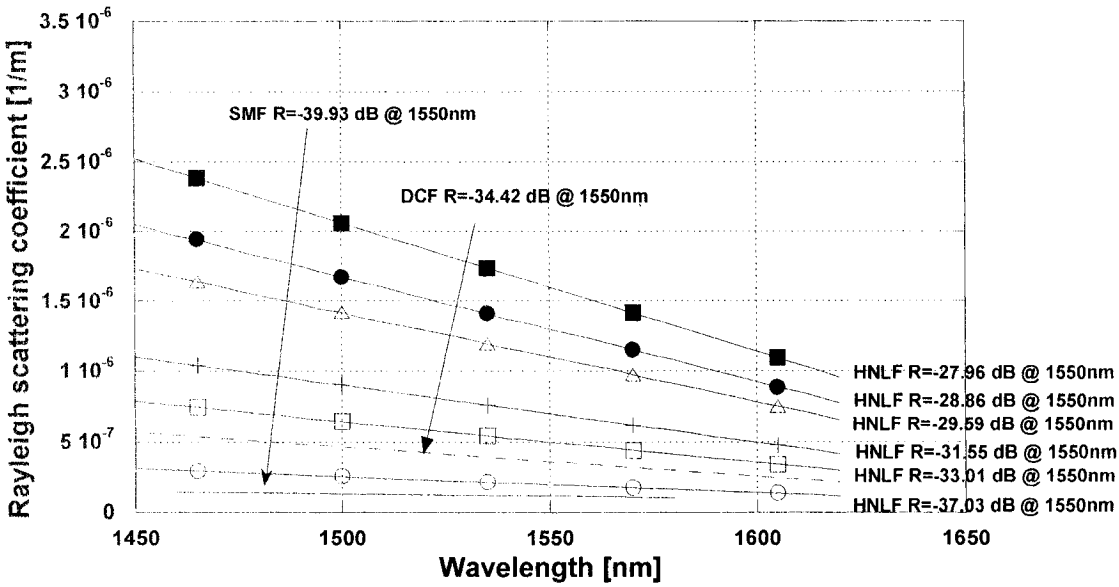

Figure a.3: fiber Rayleigh scattering coefficient of HNLF, DCF and SMF